

**THE BARNETT SHALE (MISSISSIPPIAN) IN THE CENTRAL MIDLAND
BASIN (ANDREWS, ECTOR, MARTIN, AND MIDLAND COUNTIES)**

By

CLARK H. OSTERLUND

Bachelor of Science, 2010
Baylor University
Waco, Texas

Submitted to the Graduate Faculty of
The College of Science and Engineering
Texas Christian University
In partial fulfillment of the requirements for the degree of

MASTER OF SCIENCE

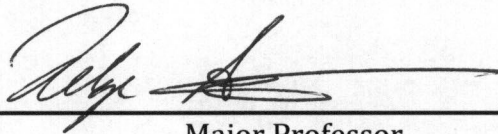
August, 2012

**THE BARNETT SHALE (MISSISSIPPIAN) IN THE CENTRAL MIDLAND
BASIN (ANDREWS, ECTOR, MARTIN, AND MIDLAND COUNTIES)**

By

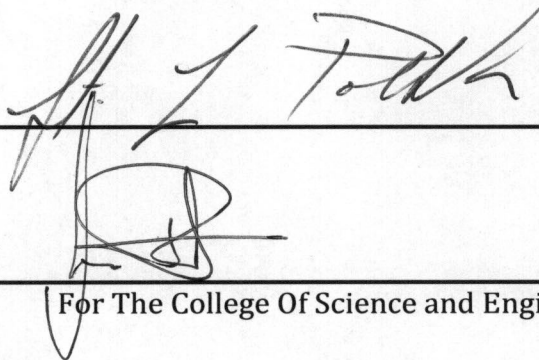
Clark Osterlund

Thesis approved:



Major Professor

R. W. Dawson



For The College Of Science and Engineering

Copyright By
Clark Harrison Osterlund
2012

ACKNOWLEDGEMENTS

First, I would like to thank Stonnie Pollock, Dexter Harmon, and the entire exploration and IT department of Fasken Oil and Ranch Ltd., whose financial backing made this project possible. I truly appreciate your interest in fostering my development as a petroleum geologist and your generous help throughout the last couple of years.

I would also like to thank my parents for motivating me throughout this process and for instilling in me the will to pursue my educational goals. In addition, I would like to thank all of my friends that I have made at TCU these past two years for putting up with me and for all the fun shenanigans we enjoyed. I have really had a blast here at TCU.

Also, I would like to thank Dr. Donovan, whose teaching style stimulated my desire to learn. I would like to thank Dr. Breyer for his initial help in getting this project off the ground. Finally, a tremendous thanks to Dr. Helge Alsleben of TCU. Your guidance and supreme editing skills has been a tremendous asset throughout this process. Your willingness to make yourself accessible to students and unwavering motivational support has made you an invaluable resource in the department.

TABLE OF CONTENTS

Acknowledgements.....	ii
List of Figures.....	iv
List of Tables.....	vi
Introduction.....	1
Previous Work.....	3
Geographic and Geologic Setting.....	4
Study Area and Methods.....	9
Division of Mississippian Strata.....	12
Lithology.....	16
Geochemistry.....	22
TOC Estimation.....	27
Age of Strata.....	29
Sediment Accumulation.....	33
Regional Context.....	46
Structure of Study Area.....	48
Discussion.....	53
Production History.....	54
Conclusions and Recommendations.....	57
References.....	59
Appendix I. Geochemical Report.....	61
Appendix II. Paleontological Reports.....	64
Vita	
Abstract	

LIST OF FIGURES

1. Major geologic features of the Permian Basin region.....	2
2. Late Mississippian paleogeographic map.....	7
3. Location of Study area within the Midland Basin.....	10
4. Type log showing stratigraphic subdivisions.....	13
5. Synthetic seismogram for Mississippian section.....	14
6. Photomicrograph of the U.B.5.....	18
7. Photomicrograph of the U.B.3.....	18
8. Photomicrograph of the U.B.2.....	20
9. Photomicrograph of the U.B.2.....	20
10. Photomicrograph of the basal U.B.2.....	21
11. Photomicrograph of the L.B.3.....	23
12. TOC wt. % vs. Depth.....	24
13. Oil potential (S2).....	26
14. TOC estimation.....	28
15. Palynological results for the Fasken Fee BM #1 SWD.....	30
16. Palynological results for the Fasken Fee BL #1 SWD.....	31
17. Palynological results for the Amoco David Fasken BS #1.....	32
18. Gross isopach map of the Mississippian section.....	34
19. Gross isopach map of Mississippian Lime.....	35
20. Cross section A-A'.....	36
21. Gross isopach map of lower Barnett.....	37
22. Type log showing >14 Ω m cutoff.....	39

23. Gross isopach map for the upper Barnett.....	40
24. Net isopach map for the upper Barnett.....	41
25. Cross section B-B'.....	42
26. Cross section C-C'.....	43
27. Gross isopach map of the U.B.2.....	44
28. Net isopach map of the U.B.2.....	45
29. Late Mississippian paleogeographic map of the Permian Basin region.....	47
30. Structure contour map on top of the Woodford Shale.....	49
31. Structure contour map on top of the L.B.3.....	50
32. Structure contour map on top of the U.B.2.....	51
33. Structure contour map on top of the U.B.6.....	52
34. Idealized deposition of bioclastic debris.....	55
35. Regional map of oil fields producing out of the upper Barnett.....	56

LIST OF TABLES

1. Wells used in the construction of cross section and for palynological analysis.....	11
2. X-ray diffraction data from the Fasken Fee BM #1 SWD well.....	17
3. Rock-Eval pyrolysis and TOC data.....	23

Introduction

The Permian Basin of west Texas and southeastern New Mexico covers more than 86,000 mi² (225,000 km²), and has produced in excess of 38 billion barrels of oil from over 3,000 fields making it the largest onshore petroleum province in the United States (Ball, 1995; IHS, 2011). The greater Permian Basin can be divided into various distinct entities. The Central Basin Platform divides the basin into two separate sub-basins with the Delaware Basin to the west and the Midland Basin to the east (Fig. 1). Stratigraphic sections from all systems of the Paleozoic are present within the basin with established production predominantly found in Pennsylvanian-Permian sections (Ball, 1995).

Mississippian strata constitute one of the least understood successions in the Midland Basin in West Texas, despite being located in a mature petroleum province. Increased activity in the “Wolfberry” (Permian) has led to a resurgence of interest in previously under-evaluated sections including Mississippian units, which have been successfully exploited for hydrocarbons in the Barnett Shale (Mississippian) in the Fort Worth Basin. Part of the ambiguity surrounding the Mississippian strata stems from lack of a general consensus on what constitutes Mississippian aged rocks. The present study examines the depositional succession and evaluates the hydrocarbon potential of Mississippian strata, which are constrained by palynology data, in the central portion of the Midland Basin (Andrews, Ector, Martin, and Midland Counties).

The Woodford, Mississippian Lime, lower Barnett, and upper Barnett formations were picked on well logs and seismic sections. These picks were incorporated in the

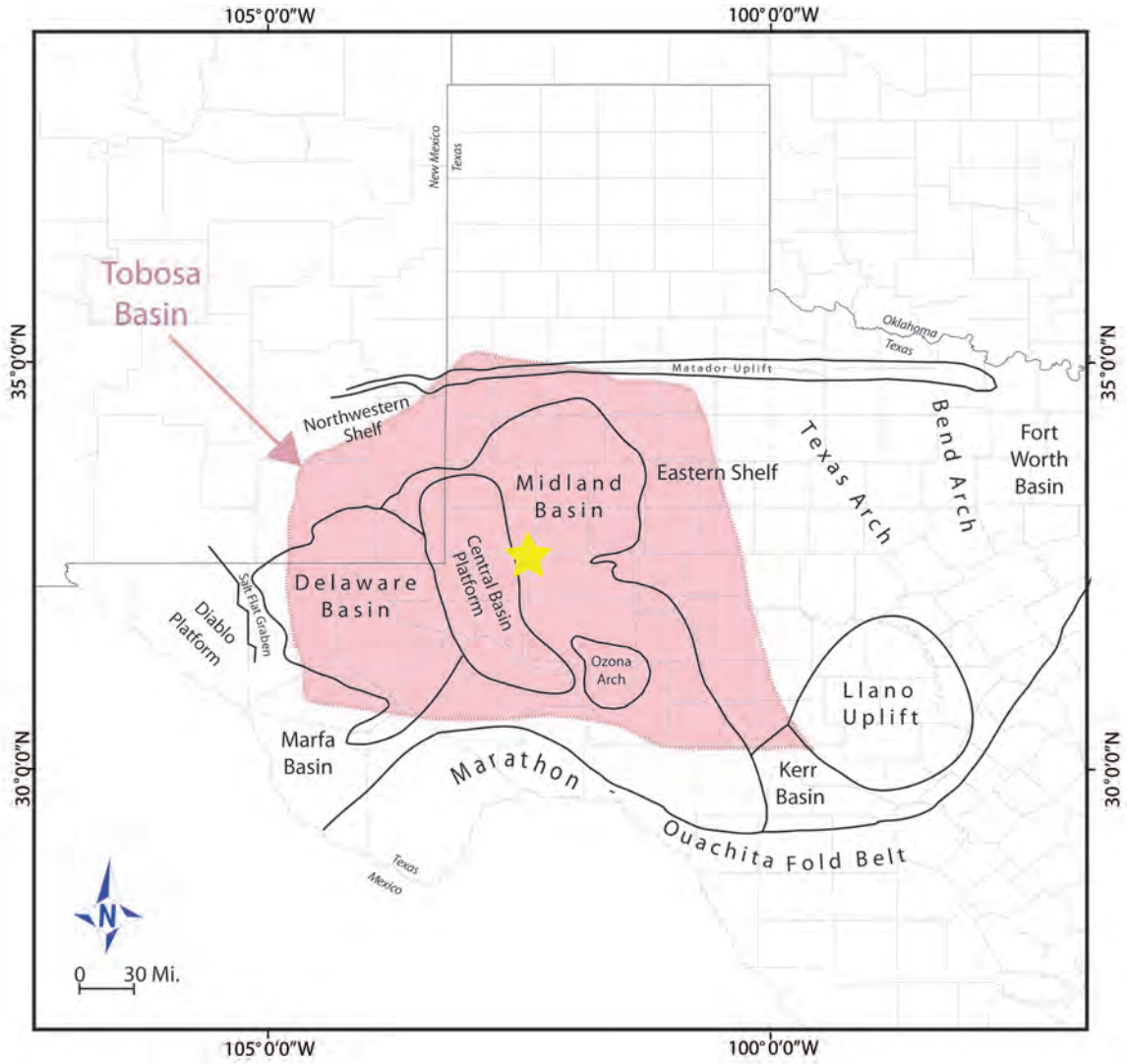


Figure 1. Regional map of the Permian Basin showing major geologic features. Yellow star shows approximate location of the study area and former maximum extent of the ancestral Tobosa Basin is shown in red (modified from Frenzel et al., 1988)

construction of cross-sections, structure maps and isopach maps, to establish the basic depositional framework of the section. The upper Barnett was studied in more detail and was further subdivided into sub-units that were also mapped. Sub-units consist of gravity flows containing more desirable reservoir properties. The results offer insight into the late stages of the evolution of the Tobosa Basin as well as late Mississippian paleogeography.

In addition to palynology data, X-ray diffraction analysis, thin sections, geochemical data, and well log analysis are used in this study. These data are used to determine the overall lithology, clay content, and organic matter in the strata. The results are related to the overall environment of deposition and are used to identify areas that warrant focus for future exploration.

Previous Work

As a reflection on the historic dearth of production out of Mississippian strata in the Midland Basin, there is scant literature concerning the overall Mississippian, let alone Barnett Shale in the subsurface. A USGS study on Mississippian Systems of the United States presents overviews on formations as well as depositional environments (Craig and Connor, 1979). A more local study provided a detailed stratigraphic description of the Mississippian strata in Gaines and Andrews Counties, Texas based on wireline logs and well cuttings (Bay, 1954). In the Delaware Basin, deposition and subsequent diagenesis of an upper Mississippian (Chesterian) oolitic shoal in Lea County New Mexico has been characterized (Hamilton and Asquith, 2000). Driven by the success of the Barnett Shale in the Fort Worth Basin, Ruppel and Kane (2006) compiled an updated overview for the

Barnett succession in the Permian Basin. Their report highlights some of the difficulties in the interpretation of Mississippian carbonates solely off of wireline logs, specifically differentiating between shallow- and deep-water facies.

While specific reports of reservoir properties are primarily found in unpublished field reports, a concise overview on late Mississippian traps in the Midland Basin is available (Candelaria, 1990). Though the succession was called “Atoka”, its use is equivocal in the report. Subsequent workers adopted the age constraints as definite (Wright, 2006), which added to the confusion about the age of the strata. The reservoir units are described as an abnormally overpressured (7,500-10,000 psi or 50-70 MPa) succession of units comprised of silty bioclastic constituents within an overall shale sequence. Faunal components within the bioclastic debris, includes fenestrate bryozoans, crinoids, ostracods brachiopods, oolites, and sponge spicules. The only published TOC values range from 1.1-4.7% TOC (Candelaria, 1990).

Geographic and Geologic Setting

The Permian Basin encompasses regions of West Texas and southern New Mexico, covering a portion of the North American craton. The Permian Basin is bounded on the north by the Matador Arch, on the east by the eastern shelf and western flank of the Bend Arch, on the south by the Marathon-Ouachita fold belt, and on the west by the Salt-Flat graben (Fig. 1) (Frenzel et al., 1988). The basin is divided into the deep Delaware Basin to the west, and the shallower Midland Basin to the east. Separating the Delaware and Midland Basins is the Central Basin Platform, which was a platform capped by carbonate reefs in the Permian (Frenzel et al., 1988). Prior to the formation of

the Permian Basin, its predecessor, the Tobosa Basin occupied a larger area. The Tobosa Basin existed from the Cambrian to the Early Pennsylvanian as a structural depression (Adams, 1965; Miall, 2008). Over that time span, the Tobosa Basin subsided and received around 7,000 feet (2,330 meters) of Paleozoic sediment (Adams, 1965).

Scant information is available on Precambrian strata as few wells penetrate basement rocks. Thus, geophysical and outcrop studies provide limited information on the nature of basement units (Hills, 1984). A gravity high associated with the Central Basin Platform is attributed to layered mafic intrusions of Precambrian age (Adams and Keller, 1996). Subaerial exposure during the early to mid-Cambrian resulted in erosion and nondeposition prior to the onset of sandstone deposition at the end of the Cambrian (Miall, 2008). In the Late Cambrian to Early Ordovician a northwestward transgressing sea occupied the area, depositing strata primarily composed of sandstone and limestone, which are mostly the carbonates of the Ellenburger Group (Adams, 1965). The Ellenburger contains limestone and dolomite members and constrains the lateral extent of the Tobosa Basin (Frenzel et al., 1988). During the Middle Ordovician, the Simpson Group was deposited. It consists of alternating layers of limestone, sandstone, and dark green shale, and does not thin over the Central Basin Platform, which was already present in Early Ordovician time. This lack of thinning has been attributed to either a quiescent period or increased subsidence of the uplift relative to the Tobosa Basin (Frenzel et al., 1988). The Simpson Group is overlain by the Montoya Formation, consisting of chert and finely crystalline carbonates. Clasts at the base of the Montoya are derived from the Simpson Group indicating an unconformity surface, although the extent of the erosional surface is unknown (Galley, 1958; Frenzel et al., 1988). During the Silurian and Early to

Middle Devonian, carbonate deposition occurred on shelf areas, with shale forming in the deeper parts of the basin. In the late Devonian-Early Mississippian, the strata that constitute the Woodford Shale were deposited in shallow anaerobic waters from a transgressing sea, forming sediments with a high organic content (Hills, 1984).

Overlying the Woodford Shale is a carbonate formation commonly referred to as “Mississippian Lime” or Lower Mississippian (Broadhead, 2009). This formation was deposited in early to mid-Mississippian. During the Mississippian, much of the southern North American continent was covered in a shallow, tropical epicontinental sea with an extensive carbonate platform (Gutschick and Sandberg, 1983). The northern portions of the Permian Basin were located on the outer margin of the platform and the southern extent has been placed in northeastern Andrews County (Fig. 2) (Bay, 1954). Minimal clastic input, coupled with warm tropical waters promoted carbonate buildups on the margins, with the extent of these carbonate buildups being largely controlled by the advancing Gondwana plate (Ruppel and Kane, 2006). In the Midland Basin, upper Mississippian units were deposited as fine-grained clastic sequences containing interbedded carbonates. Proximal to the shelf margins, shale comprises the majority of strata deposited during Osagean-Meramecian time, while carbonate deposition dominated during the Chesterian (Hamilton and Asquith, 2000). Distal to the shelf margin, hemipelagic shale predominates the Mississippian units, with carbonate debris transported episodically to the basin. In the mid-late Mississippian, the outer portions of the advancing Ouachita trough had been uplifted, resulting in siliciclastic sediment being shed off northward into the basin (Ruppel and Kane, 2006).

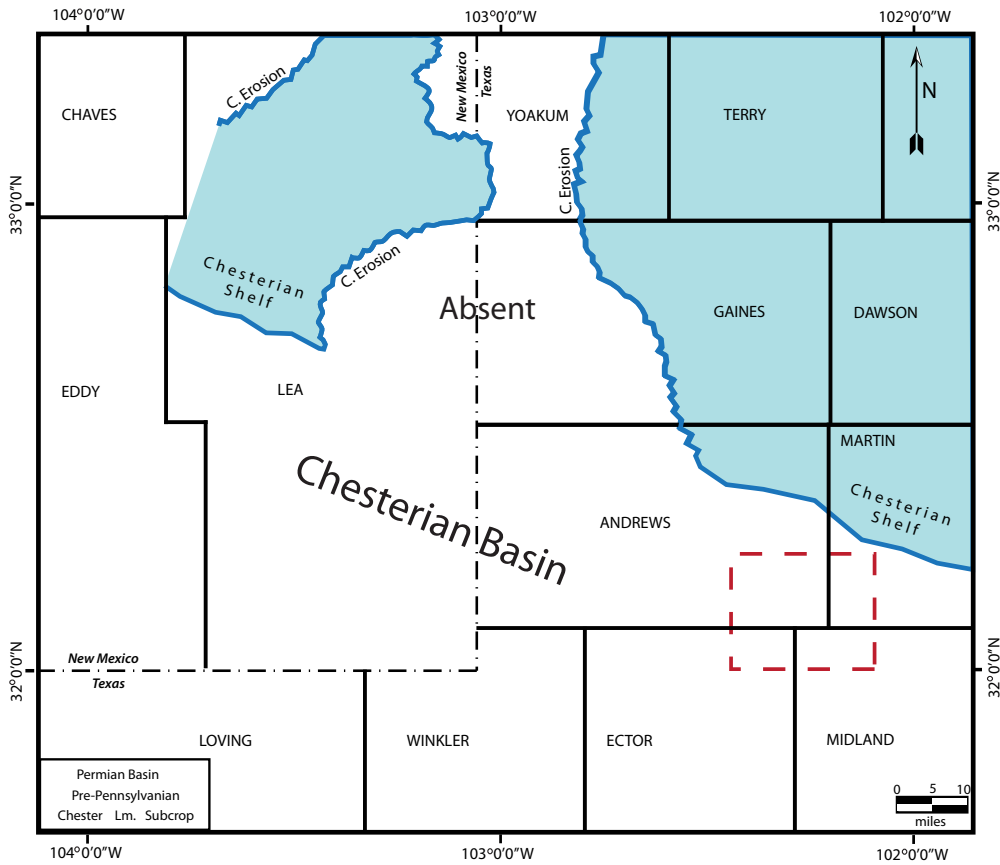


Figure 2. Map showing the approximate location of Late Mississippian (Chesterian) shelf. Subsequent erosion over the Central Basin Platform is shown. Dashed red square outlines the study area. Figure is modified from Hamilton and Asquith (2000).

The Tobosa Basin ceased to be a single depositional entity in the Early Pennsylvanian, a result of uplift of the Central Basin Platform, and the subsequent subsidence of the Delaware and Midland Basins (Ye et al., 1996). The Strawn, Canyon, and Cisco Formations are present above the late Mississippian-early Pennsylvanian shale sequence in the Midland Basin. The dominant feature of the Pennsylvanian geology in the Midland Basin is the Horseshoe Atoll, formed by sequences of Strawn, Canyon, Cisco, and early Permian carbonates. An increase in subsidence in the latter stages of the Pennsylvanian promoted the buildup of carbonates along the basin edges, deterring clastic sedimentation in the basin and resulting in a starved basin environment (Adams et al., 1951).

During the Permian, subsidence continued with average rates of subsidence, exceeding 200 m/Ma (Scholle, 2006). Permian strata within the Permian Basin are characterized by an overall progradation of various types of depositional environments including sabkhas, open marine shelves, and shelf-edge organic buildups (King, 1948; Frenzel et al., 1988; Miall, 2008; Scholle, 2006). In the Midland Basin, sediment gravity flow processes and submarine fan systems carried sand, shale, and carbonates into the basin (Scholle, 2006). The later stages of the Permian (Ochoan) are marked by the initiation of a barred basin to the west and the subsequent deposition of thick evaporite deposits (Miall, 2008).

As a result of a sustained oceanic regression following the end of the Permian, substantial amounts of Upper Permian strata (hundreds of feet/meters) were eroded (Hills, 1984). Triassic deposition resulted in the formation of continental red beds in both

the Midland and Delaware basins. Jurassic and Lower Cretaceous rocks are present in the basins, presumably the result of subaerial exposure (Hills, 1984). Upper Cretaceous limestone and sandstone are also present. In the Tertiary, uplift associated with Basin-and-Range deformation caused the western side of the Permian basin to be exhumed, resulting in the present exposures along the western margins of the Delaware Basin.

Study Area and Methods

The study area is located in the central portion of the Midland basin, covering approximately 25 mi² (65 km², Fig. 3). The area includes the southeastern portion of Andrews County, the northeastern portion of Ector County, the northern region of Midland County, and the southwestern region of Martin County. It extends from the basin axis to the eastern flank of the Central Basin Platform. 130 well logs from wells that penetrate all or portions of the Mississippian section were used in this study. Well logs from the Fasken Fee BM #1 SWD well, located in the southern region of the study area served as the type log (Fig. 3).

A three-dimensional seismic volume covering a portion of the study area (Fig. 3) was interpreted to increase control on structure maps. Thirteen wells are present containing sonic logs (Δt) in the confines of the seismic survey. Synthetic seismograms were generated using a Δt log, and then paired with the actual seismic trace at the well location. The synthetics were stretched and squeezed using anchor points to accomplish as high a correlation match as possible. However, not all subdivisions contained sufficient acoustic impedance to warrant picking (see below). Horizons that did were gridded and then converted to depth to be incorporated in the construction of structure

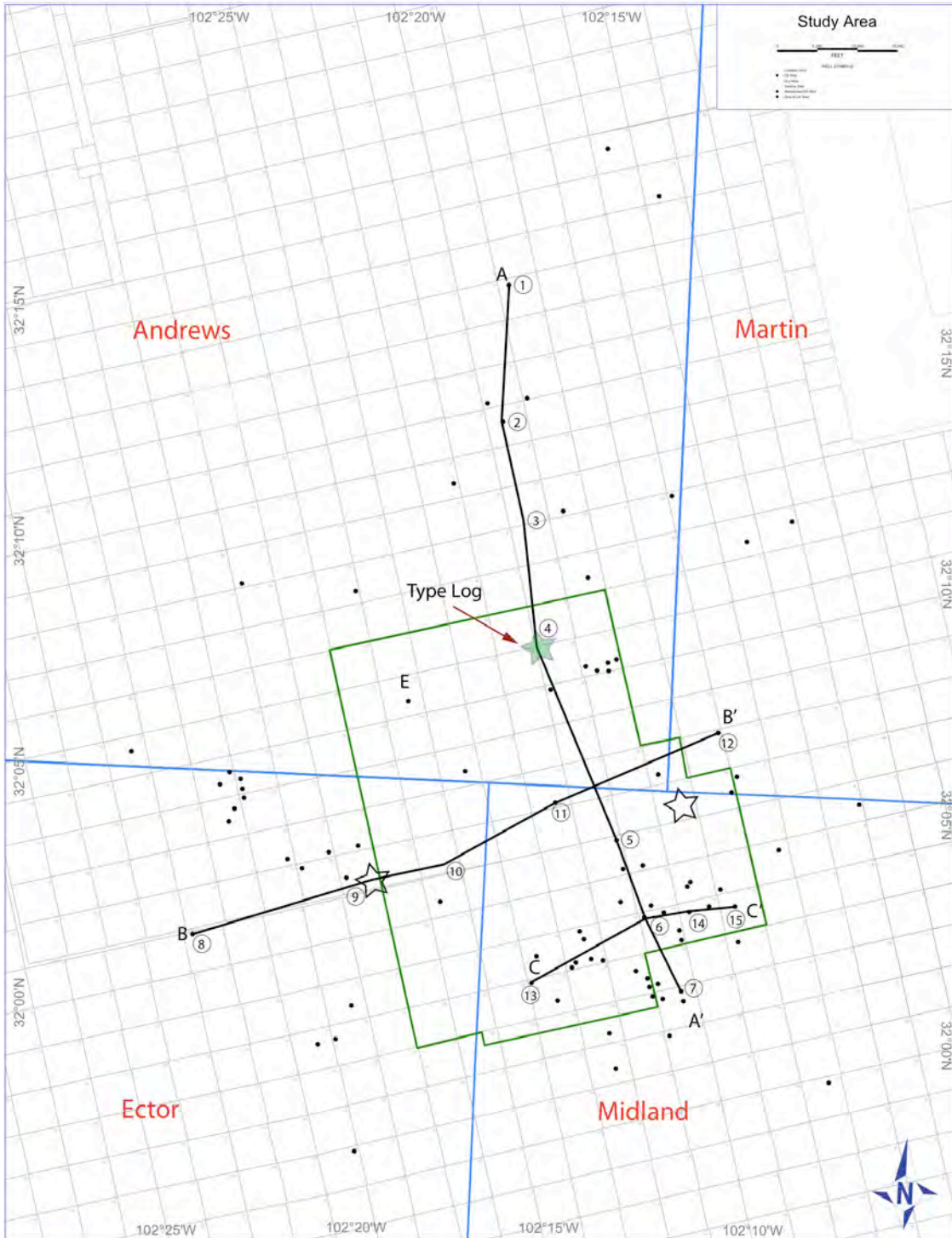


Figure 3. Map showing the location of the study area within the Midland Basin. Map also depicts the location of the type log (green star) and cross sections constructed for the study. See table 1 for the wells used in constructing the cross sections. White stars correspond to wells from palynology data was obtained.

Table 1. Wells used in the construction of cross sections. Type log highlighted in yellow. Asterisk (*) corresponds to wells with available palynology data. AOIL- Abandoned oil well, SWD-Salt water disposal well.

Well	UWI (API Num.)	County	Well Name	Well Number	Operator	WELL TD	Status
1	42-003-4006800	ANDREWS	MABEE RANCH 14	1	FASKEN OIL AND RANCH LTD	13370	OIL
2	42-003-3077900	ANDREWS	FASKEN BLK /BB/	2	MOBIL OIL CORP	13500	AOIL
3	42-003-1031100	ANDREWS	FASKEN DAVID AZ	1	PAN AMERICAN	13600	DRY
4*	42-003-4216900	ANDREWS	FEE BM	1 SWD	FASKEN OIL AND RANCH LTD	14200	SWD
5	42-329-3126400	MIDLAND	CASSELMAN 4	1	U S OPERATING INC	13675	AOIL
6	42-329-3131700	MIDLAND	FASKEN	4015B	FASKEN OIL AND RANCH LTD	13520	OIL
7	42-329-3128400	MIDLAND	SCHARBAUER	2-27	ENDEAVOR ENERGY RESOURCES	13352	OIL
8	42-135-1071100	ECTOR	SUPERIOR-RATLIFF	1	FASKEN DAVID	13335	AOIL
9*	42-135-4134700	ECTOR	FEE BL	1	FASKEN OIL AND RANCH LTD	14568	SWD
10	42-135-3458900	ECTOR	FASKEN 16	1	ANSCHUTZ CORP	13758	DRY
11	42-329-0200600	MIDLAND	FEE X	1	DAVID FASKEN	12714	AOIL
12	42-317-3282600	MARTIN	COWDEN	1	L & B OIL CO INC	13570	AOIL
13	42-329-3118100	MIDLAND	GETTY-FASKEN	1-19	ANSCHUTZ CORP	13697	AOIL
14	42-329-3148600	MIDLAND	BARRON	414	EXXON CORPORATION	12128	AOIL
15	42-329-3151400	MIDLAND	FASKEN D	613	EXXON CORPORATION	11700	AOIL

maps. Structure contour maps were constructed to show depths to the top of the Woodford Shale and Mississippian divisions. Isopach maps and cross sections were constructed to decipher patterns of sediment accumulation in the area.

Cuttings taken from the Fasken Fee BM #1 SWD well were submitted to Gerald Waanders (Independent Palynologist) for palynological analysis. The ability to assign a tentative age to the strata aids in the overall depositional interpretation as Late Mississippian to Early Pennsylvanian paleogeography varied. In addition to cuttings, GeoSystems LLP. completed X-Ray diffraction analyses and determined the total organic carbon (TOC) content on nine side wall cores. XRD analyses quantitatively apply weight percent values to various mineral phases, and offers insight into clay type present in the strata.

Division of Mississippian Strata

“Mississippian”, as used in this study, corresponds to the strata extending from the low gamma ray response denoting the top of Silurian-Devonian carbonates to the lowermost portion of the overlying “Atoka Lime” carbonate (Pennsylvanian) (Fig. 4). On seismic, the Woodford is expressed as a trough, overlying a sharp peak denoting the top of the Silurian-Devonian carbonates (Fig. 5). A limestone formation commonly referred to as the “Mississippian Lime” or “Lower Miss” is present atop the Woodford Shale Formation (Ruppel and Kane, 2006). The top of the Mississippian Lime is denoted by an abrupt suppressed gamma ray response, a function of the carbonate present beneath the overlying shale. On seismic, the Mississippian Lime appears as a basal portion of a peak. The remaining section between the Mississippian Lime and Atoka Lime is deemed

420034216900



FASKEN
FEE BM
1 SWD

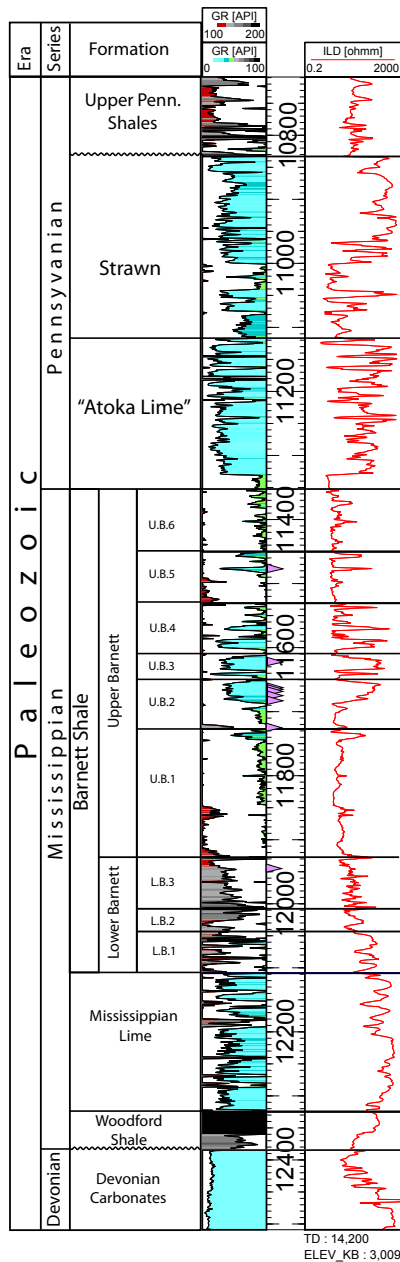


Figure 4. Type log showing stratigraphic subdivisions utilized. Purple triangles denote sidewall core locations

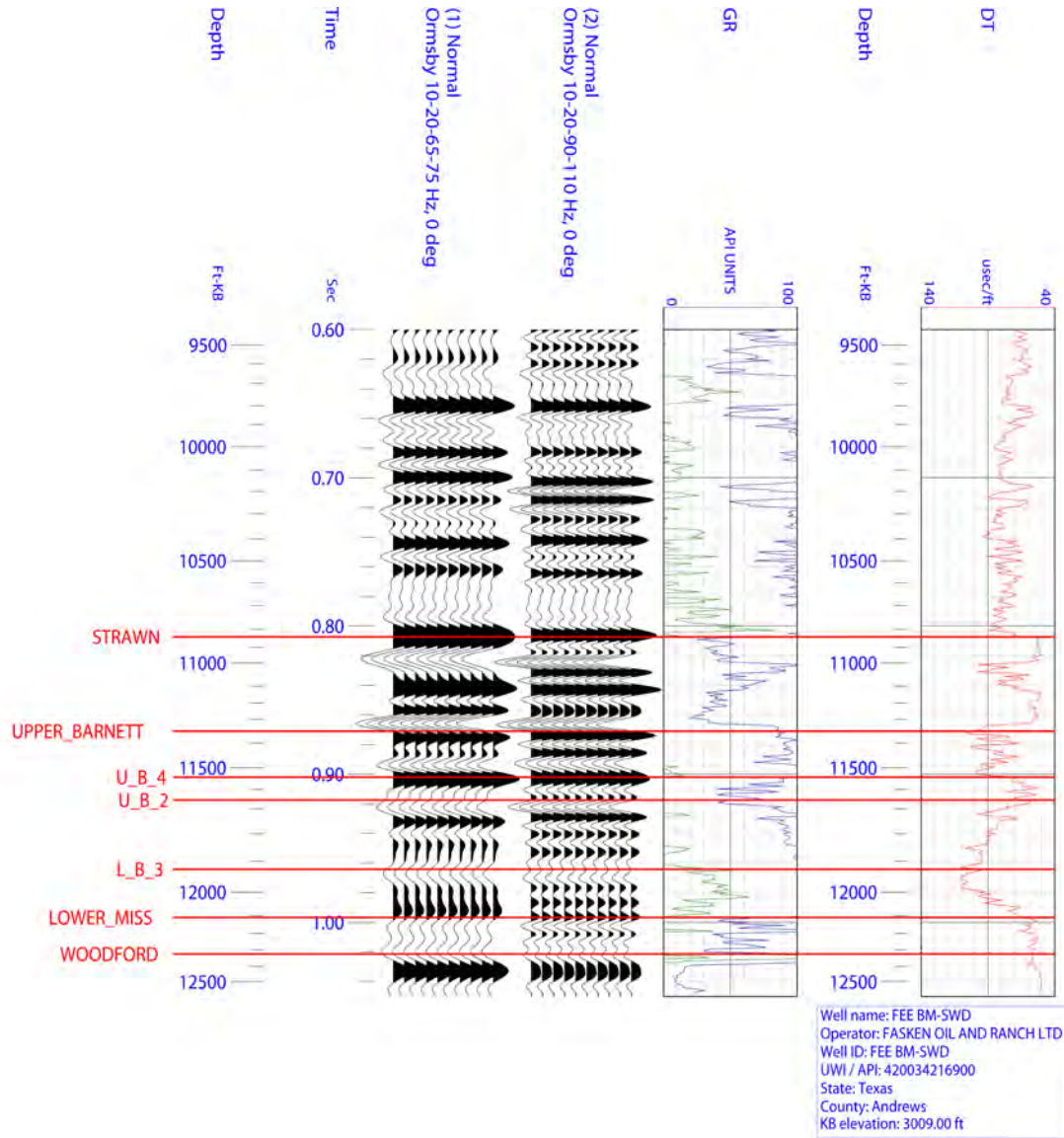


Figure 5. Synthetic seismogram for the Mississippian section displaying horizons incorporated in the construction of structure maps.

Barnett Shale, which can be further subdivided into an upper and lower section.

Extending from the “Mississippian Lime”, the lower Barnett is on average 180 feet (55 meters) thick, is characterized by high gamma ray measurements and is associated with resistivity spikes ($>10 \Omega\text{m}$). The lower Barnett was divided into 3 subdivisions (L.B.1 through L.B.3). L.B.1 lies directly above the Lower Mississippian. The top of L.B.1 is expressed by a thin (<10 feet, 3 meter) occurrence of a low gamma ray excursion along with an abrupt decrease in resistivity. L.B.2 is an overall fining upward succession that culminates with both a sharp increase in gamma ray (>180 API) and resistivity ($>150 \Omega\text{m}$) values. The top of the lower Barnett, L.B.3 is expressed as a sharp gamma ray peak coupled with a resistivity excursion on the order of 90-200 Ωm . The top of the lower Barnett is shown to have a trough for a seismic signature.

The upper Barnett section is divided into six intervals (U.B.1 through U.B.6) on the basis of clean gamma ray signatures, representative of an amalgamation of silty bioclastic debris encased in shale. Overlying the lower Barnett, U.B.1 is comprised of a calcareous-siliceous shale sequence the top of which is denoted by an excessively high GR and resistivity excursion of >160 API and 90 Ωm , respectively. U.B.2 and U.B.3 comprise the thickest intervals in the upper Barnett, and display a coarsening upward, funnel shaped gamma ray electrofacies, along with a spike in resistivity. U.B.2 is representative of a small trough on seismic. U.B.4 and U.B.5 are thinner, yet still maintain a pronounced clean gamma ray and associated resistivity spike. U.B.4 contains a strong peak as a seismic signature. The U.B.6 is picked by a subtle clean kick in the gamma ray response associated with a resistivity spike and the top of a peak on seismic.

Overlying the Barnett is a formation termed “Atoka Lime”, equivalent to the “Bend Group” (Wright, 2006).

Lithology

Nine sidewall cores from the Mississippian section in the Fasken Fee BM #1 SWD well were submitted to GeoSystems for X-ray diffraction (XRD) analysis (Fig. 4; Table 2). Eight cores were from the upper Barnett interval, specifically the U.B.5, U.B.3, and U.B.2 intervals, with the remaining core taken from the lower Barnett. All but one core from the upper Barnett was taken from the sections coinciding with the cleaner gamma ray values.

U.B.5 is a light gray, sandy, fossiliferous, coarse-grained dolostone (Fig. 6). Layering is observed in the form of variations in grain size, and in the semblance of bioclastic grains. Bioclastic grains are moderately sorted and include fragmented brachiopods and echinoderms with a size greater than 1.0 mm. Fragmentation of the carbonate constituents in the U.B.5 as well as the underlying subdivisions supports the notion that these bioclasts have been transported from their original environment of deposition. Apatite is present in the sample (9 weight %) in the form of replaced bone fragments as well as nodular form. Total clay content derived from XRD is around 3 weight %, equally comprised of illite, kaolinite, and chlorite. Quartz comprises 22 weight % of the sample. Carbonate minerals include ferroan dolomite (52 weight %) and 12 weight % of calcite (Table 2).

The sample taken from U.B.3 is comprised of a dark gray oolitic carbonate grainstone (Fig. 7). XRD results show that the rock contains 85% carbonate by weight

Table 2. X-ray diffraction data for the Fasken Fee BM SWD #1 showing weight % of various minerals present. See Figure 3 for location of well, and Figure 4 for intervals sampled

X-RAY DIFFRACTION ANALYSIS

Fee BM No. 1 SWD Well

SUB-UNIT	SAMPLE DEPTH (ft)	CLAY MINERALS						OTHER MINERALS						CARBONATE MINERALS				DRILLING MUD SOLIDS				TOTALS			SAMPLE NUMBER		
		SMECTITE	ILLITE-SMECTITE	ILLITE	KAOLINITE	CHLORITE	REICHWEIFE ORDERING	ILLITE-SMECTITE EXPANDABILITY %	QUARTZ	K-FELDSPAR	PLAGIOCLASE	PYRITE	ANHYDRITE	APATITE	FERRONAN DOLOMITE	CALCTE	DOLOMITE	SIDERITE	OTHER CARBONATES	BENTONITE	HALITE	BARITE	OTHER SOLIDS	TOTAL CLAY MINERALS		TOTAL OTHER MINERALS	TOTAL CARBONATES
U.B.5	11477	<1	1	1	1	1	R0	20	22	<1	2	2	9	52	12								3	33	64	0	003
U.B.3	11625	<1	<1		3	R0	25	6		4	1		1	7	75	3							3	12	85	0	006
	11662	1	2	1	<1	R0	15	19		2	1		4	68	2								4	22	74	0	008
	11665	3	5	<1	1	R0	20	42		2	1		<1	4	35	7							9	45	46	0	009
U.B.2	11669	1	4	1	<1	R0	20	45		3	1	1	<1	5	27	12							6	50	44	0	010
	11677	6	6	2	3	R0	30	53	<1	1	2		1	5	19	2							17	57	26	0	011
	11683	4	4	7	6	R0	20	46		2	2		<1	2	27								21	50	29	0	013
	11724	5	20	6	7	R0	20	19		1	3	4	9	6	17	3							38	36	26	0	015
L.B	11946	8	46	4	5	R0	20	28		1	3	4	1	<1	<1	<1						63	37	Tr	0	018	

Reichweite is the probability that in mixed layer clay, given a layer of clay A, the adjacent layer is clay B.

R = 0 is a random mixing of layers

R = 1 is short range ordering

R = 3 is long range ordering

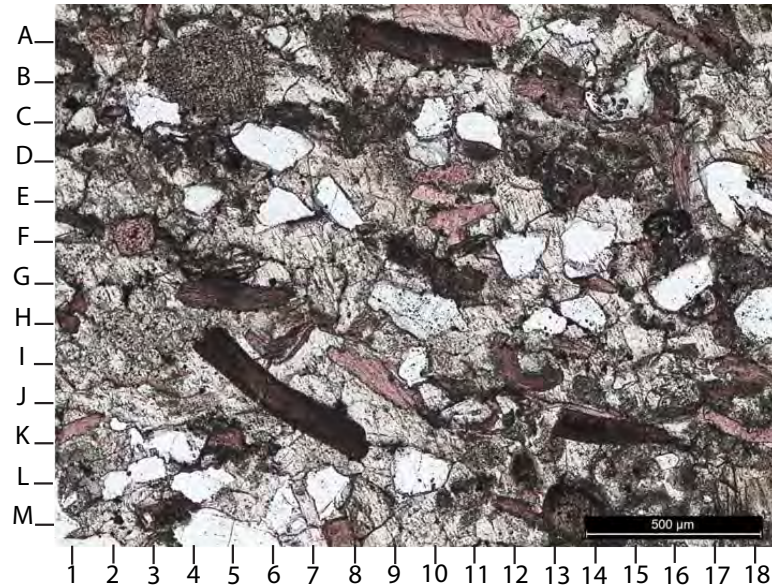


Figure 6. Photomicrograph representative of the sample taken from the U.B.5. Components include quartz grains (e.g., D6), and a range of bioclastic fragments. Fragments include brachiopods (e.g., G5), bivalves (e.g., A11), and echinoderms (e.g., F3).

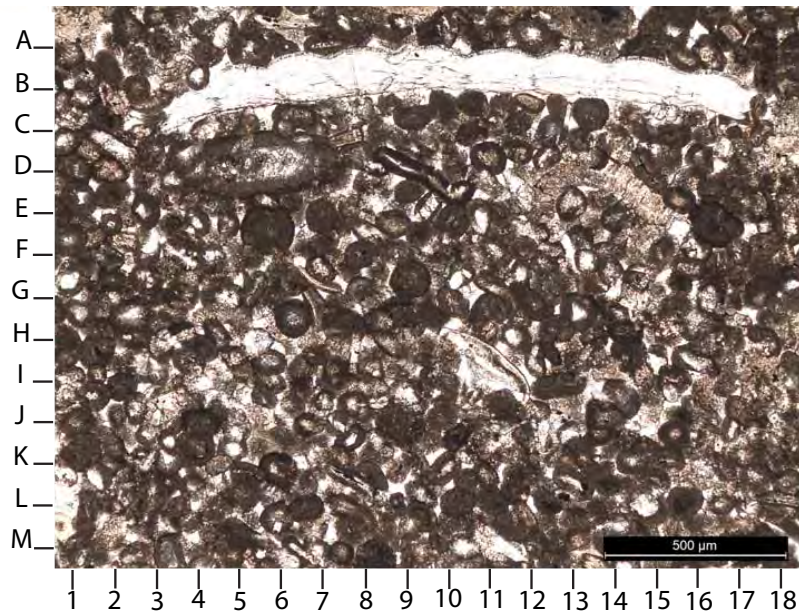


Figure 7. Photomicrograph of the fossiliferous ooid grainstone of the U.B.3. Abundant ooids are present (e.g., E6, H6) as well as brachiopod fragments (e.g., B11).

(Table 2) that occurs predominantly in the form of calcite present in ooids and as intergranular cement. A more diverse faunal assemblage is present than in the U.B.5, including ooids, brachiopods, echinoderms, bryozoans, ostracods, and bivalves (Fig. 7). Overall the interval is well sorted with grains ranging from 0.08-0.11mm. Terrigenous material in the cores of the ooids makes up 10 weight % of the rock (6 weight % quartz silt and 4 weight % plagioclase). Chloritic clays constitute 3 weight % of the rock.

Five samples were chosen from the U.B.2 section, which reveals that the clean GR response is the result of a fine-grained, dark gray limestone interval (Figs. 8 and 9). Extensive bioturbation in the interval could have aided in the destruction of any bedding structures present at time of deposition. Observed faunal elements are similar to the overlying detrital sections consisting of bivalves, ostracods, echinoderms, and ooids. Carbonate minerals (by weight %) account for a majority of the rock. Carbonate is present as calcite, dolomite, and ferroan dolomite. Though abundant, carbonate decreases with depth from 74% to 29%. Terrigenous mineral phases are also pervasive in the rock with quartz comprising 19-53% of the rock by weight. Trace amounts of plagioclase silt (1-3% by weight) are also present. Clay content accounts for 5-21 weight % of the rock and increases with depth. Clay is present in the form of illite-smectite (1-21%), illite (2-6%), kaolinite (1-7%), and chlorite (1-6%).

The basal portion of U.B.2 is a poorly sorted calcareous and phosphatic shale (Fig. 10). Compared to the overlying strata, this section contains higher clay content (38 weight %), including illite (20%), chlorite (7%), kaolinite (6%), and some mixed layer illite-smectite (5%). Terrigenous constituents account for approximately one quarter of

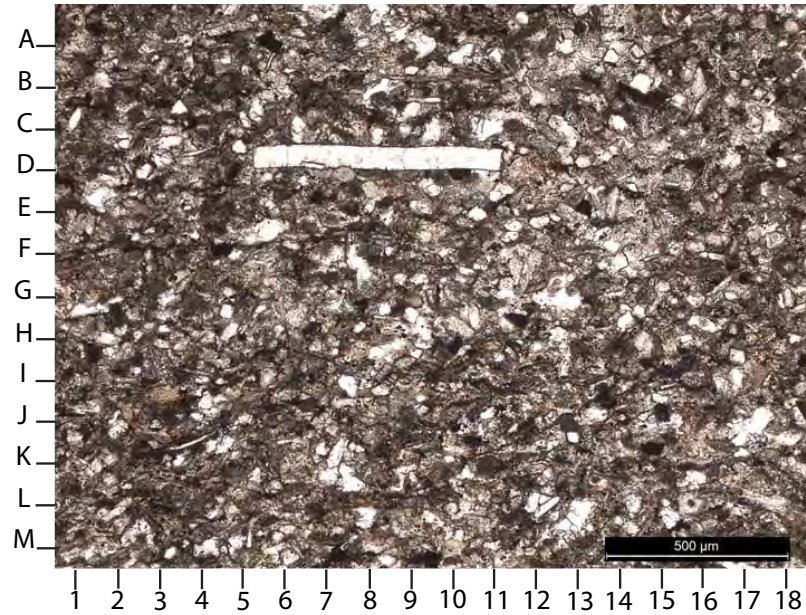


Figure 8. Photomicrograph of sample taken from the U.B.2 displaying a large bivalve fragment (D8) as well as siliciclastic grains (e.g., E6).

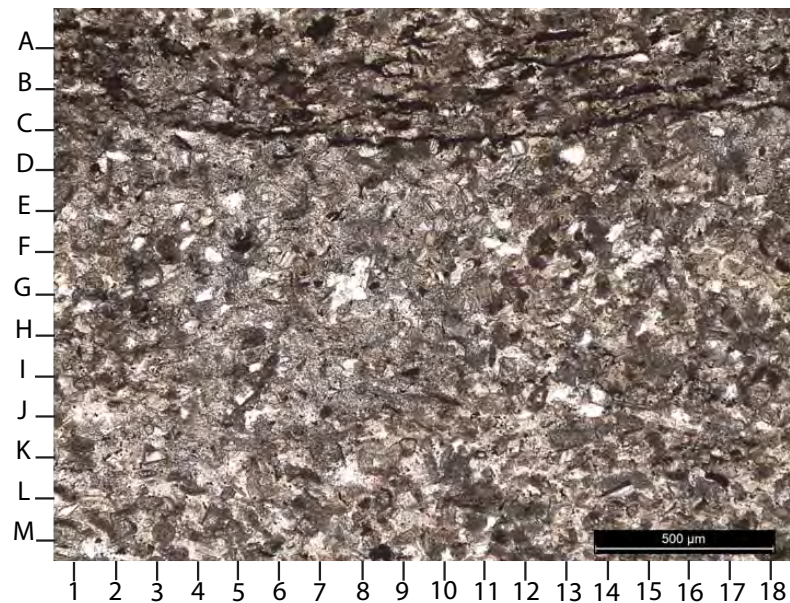


Figure 9. Photomicrograph of sample taken from the U.B.2 showing a stylolite (C3-C18) separating two distinct textures of rock. An argillaceous texture is found above a more siliciclastic, silt-rich carbonate texture.

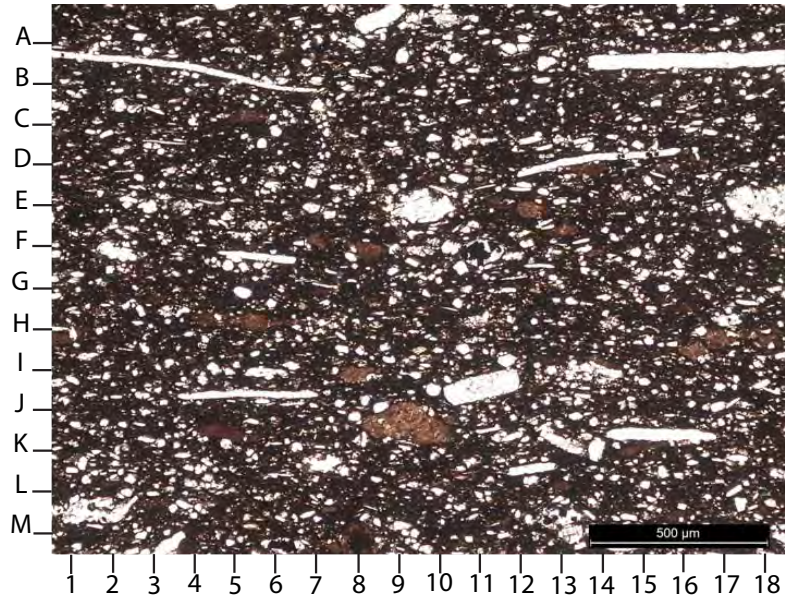


Figure 10. Photomicrograph of sample taken from the basal portion of the U.B.2 displaying a dark clay rich matrix with scattered bioclastic fragments (e.g., A16, B5).

the rock by weight. Quartz comprises 19 % weight and minor amounts of plagioclase (3%) and potassium feldspar (1%) are present. Carbonate minerals also comprise ~25% of the rock. Calcite in the form of bioclastic debris and as fossil fragments comprises 17 weight %. Dolomite (3%) and ferroan dolomite (6%) are also present as artifacts of diagenesis. Other minerals that formed as a result of diagenesis are apatite (9 weight %) and pyrite (4 weight %). Unpublished mudlogs have previously attributed this portion of the U.B.2 coinciding with the elevated gamma ray and resistivity response as being a coal. This interpretation, however, appears unlikely. The bulk density for a coal is typically 1.2-1.8 g/cm³ (Serra, 1990), whereas in the study area, bulk densities for the section of interest are on the order of 2.3-2.4 g/cm³.

The sample taken from the lower Barnett is a silty shale (Fig. 11). Clays dominate the rock and comprise 63 weight %. Illite is the most prevalent clay mineral (46%) with the remainder comprised of mixed layer illite-smectite (8%), chlorite (5%), and kaolinite (4%). Terrigenous components account for little of the overall weight percent with only plagioclase (3%) and potassium feldspar (1%) present. Quartz makes up 28% of the rock primarily as a result of recrystallization. Carbonates are scarce in the lower Barnett with ferroan dolomite the sole phase present contributing <1 weight %.

Geochemistry

The same samples subjected to XRD were also analyzed for total organic carbon (TOC) content. Samples taken from the upper Barnett contain relatively low values (<1 weight % TOC), although an overall increase is seen with depth from 0.04-0.38 weight % (Table 3) (Fig. 12). The overall dearth of TOC present in the upper Barnett samples is

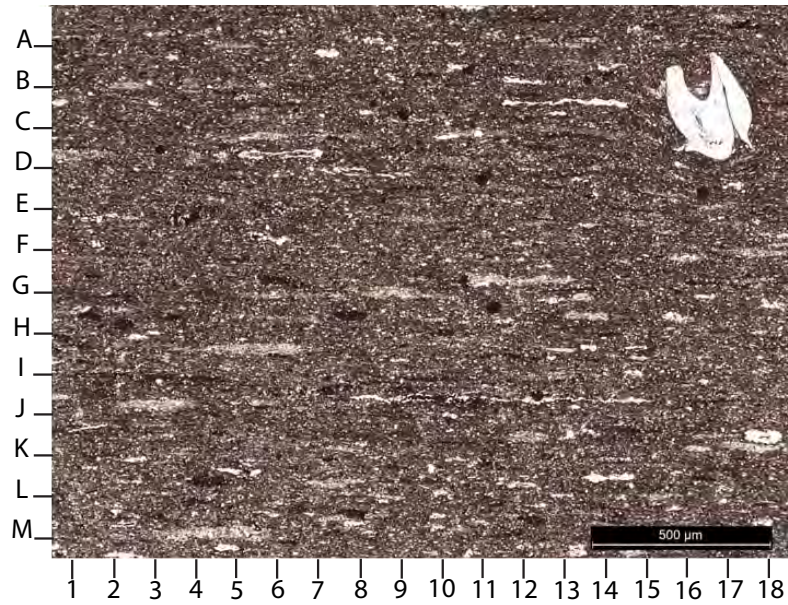


Figure 11. Photomicrograph of sample taken from the L.B.3 showing the overall texture of the rock. Bioclasts (e.g., B17) are scarce. Light horizontal masses are clay probably from the backfill of feeding traces.

Table 3. Rock-Eval pyrolysis data for the Fasken Fee BM #1 SWD well.

GeoSystems - Ctruck Segment												BM SWD #1
Source Rock Analysis												
Formation Name	Depth (ft)	Leco TOC (wt% HC)	Rock-Eval S1 (mg HC/g)	Rock-Eval S2 (mg HC/g)	Rock-Eval S3 (mg CO2/g)	Tmax (°C)	Hydrogen Index (32x100/TOC)	Oxygen Index (33x100/TOC)	S2/S3 Conc. (mg HC/mg CO2)	S1/TOC Norm Oil Content	Production index (21/31+32)	Experimental Notations
U.B.5	11,477	0.26	0.04	0.01	0.11	0	4	42	0	15	0.80	
U.B.3	11,625	0.26	0.29	0.08	0.14	0	31	54	1	112	0.78	
U.B.2	11,662	0.38	0.58	0.32	0.16	0	84	42	2	153	0.64	
U.B.2	11,665	0.45	0.86	0.42	0.21	365	93	47	2	191	0.67	Low Temp S2 Shoulder
U.B.2	11,669	0.31	0.15	0.13	0.05	0	42	16	3	48	0.54	
U.B.2	11,677	1.12	0.38	0.67	0.13	463	60	12	5	34	0.36	
U.B.2	11,683	0.82	0.29	0.43	0.08	464	52	10	5	35	0.40	
U.B.2	11,724	4.65	3.56	5.57	0.37	461	120	8	15	77	0.39	Low Temp S2 Shoulder
L.B.3	11,946	5.31	4.88	5.45	0.27	458	103	5	20	92	0.47	Low Temp S2 Shoulder

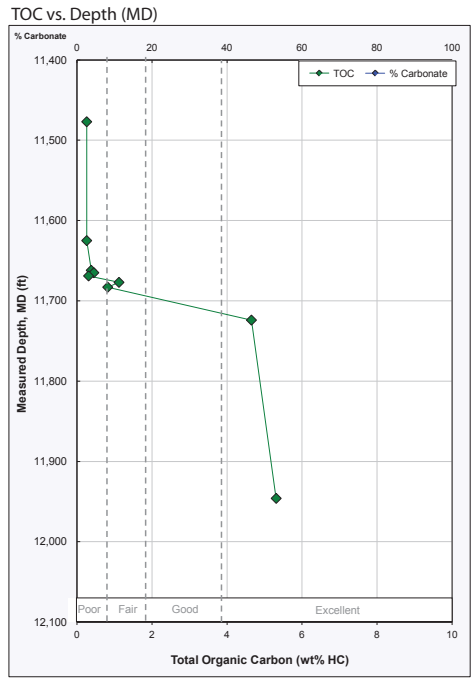


Figure 12. TOC (weight %) vs. depth (MD)

expected, in that they were taken from mass gravity deposits comprised of carbonate debris, not an organic rich mudstone. The basal portion of the U.B.2. contains 4.65 weight %, whereas the lower Barnett contains the highest TOC value among the samples (5.3 weight %). These values overlap with values ranging from 1.1-4.7 weight % TOC south of the study area (Candelaria, 1990). In the neighboring Delaware Basin, TOC values have been found to be on the order of 4.4 weight % (Kinley, 2006).

As part of the Rock-Eval Pyrolysis, samples were heated to determine how much petroleum has already been generated and how much generation potential is remaining. At approximately 572°F (300°C) previously generated hydrocarbons in the source rock are expelled creating a peak and the content of the hydrocarbons coinciding with the numbers C1-C25 are recorded. The values for S1 correspond to the area beneath the peak, representative of hydrocarbons that have already been produced in the rock and failed to migrate out (Bjorlykke, 2010). A subsequent peak (S2) forms as the sample is subjected to 1022°F (550°C). This second peak represents the samples ability to continue to generate hydrocarbons.

Samples taken from the gravity flows contained paltry S1 values ranging from 0.04 to 0.29 mg HC/g (Table 3) (Fig. 13). S2 values for the upper gravity-flows are also low, while increasing with depth from 0.11 to 0.67 mg HC/g. Samples taken from the U.B.2 and the lower Barnett Shale contain heightened values. The U.B.2 shale sample has a S1 value on the order of 3.56 mg HC/g, and an S2 value of 5.57 mg HC/g. The lower Barnett contains the highest S1 value (4.88 mg HC/g) out of all samples and an S2 value of 5.45 mg HC/g.

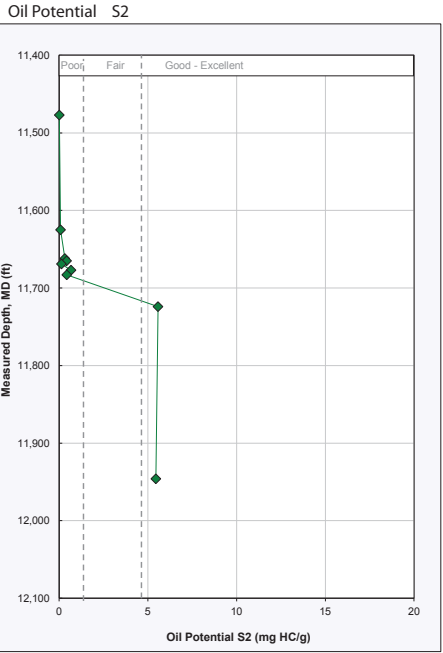


Figure 13. Oil potential (S2) vs. Depth (MD)

TOC Estimation

TOC content can be obtained indirectly from the inverse relationship of the gamma ray (GR) and true resistivity (Rt) curves (Heslop, 2010). This method was used to estimate TOC rich sections in the study area. The method calls for the curves to be plotted on the same track with one of the scales reversed. In a non-source shale (TOC lean) the curves tend to track, whereas in a source shale (TOC rich) separation of the curves will occur. The separation is achieved because both of the logs increase in value.

A GR scale of 175-50 API units and a resistivity logarithmic scale of 0.5-500 Ωm were applied to wells containing suitable curves. The results reveal that the upper Barnett section is relatively TOC lean, whereas the greater separation between the two curves in the lower Barnett section suggests higher TOC concentrations (Fig. 14).

To apply a quantitative value to the degree of separation the following formula, modified from Heslop (2010) was used (Fig. 14):

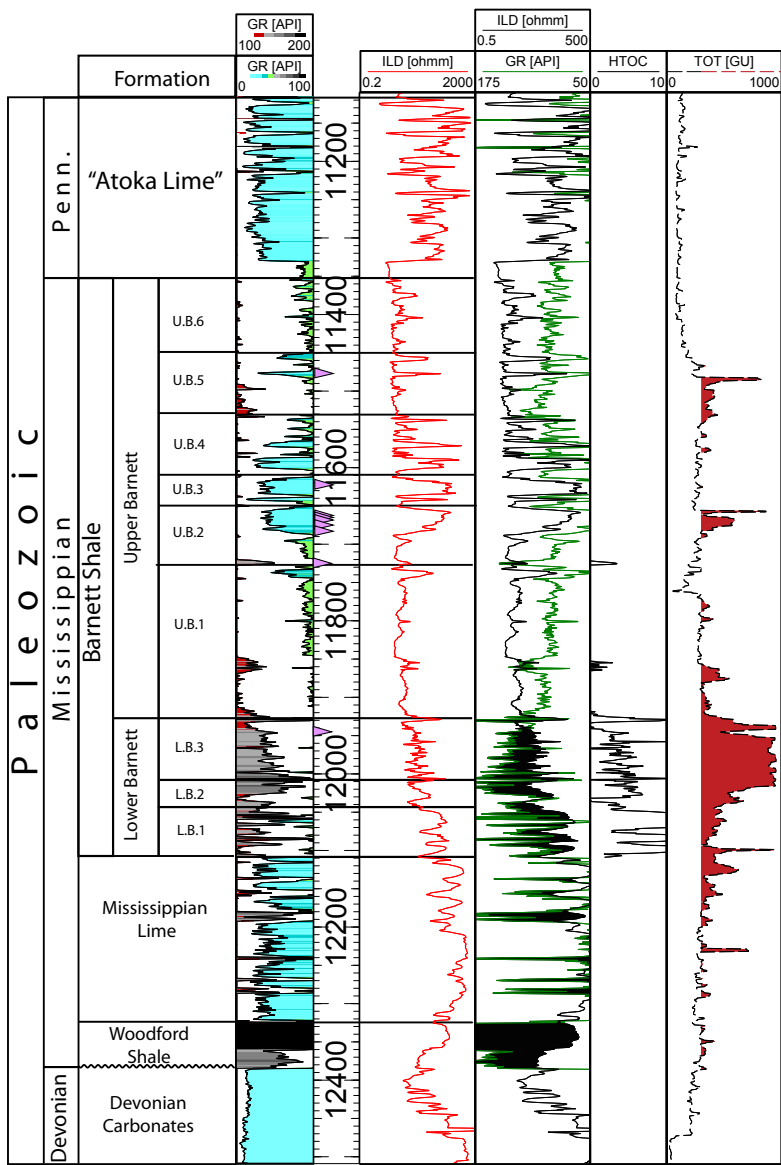
$$\text{Equation 1: } TOC = (\Delta GR + \Delta Rt) * 30 / (GR_{TOC} + \log_{10}(Rt_{TOC})),$$

where ΔGR and ΔRt are the separation of the curve from the base line, GR_{TOC} is representative of the respective log values present in the area of separation, and a value of 30 is applied to scale the separation. GR_{TOC} and Rt_{TOC} are TOC values originally calibrated to lab obtained TOC values.

420034216900



FASKEN
FEE BM
1 SWD



TD : 14,200
ELEV_KB : 3,009

Figure 14. Example of TOC estimates using the Heslop method described above. Notice how the curves track each other in the upper Barnett section, whereas separation occurs in the lower Barnett. TOT= Total gas content observed from the mudlog, HTOC= the TOC curve generated from equation 1.

Age of Strata

Historically, fields producing from the bioclastic debris flows within the upper Barnett have been reported as Mississippian (Chesterian) or Pennsylvanian (Atokan) in age. R.V. Hollingsworth (Unpublished Paleontological Reports) identified the “Atoka Lime” on the occurrence of Atoka fusulines. Underlying the “Atoka Lime”, Hollingsworth placed the top of the Barnett Shale on the basis of a color change in conjunction with a change in lithology, due to an absence of fusulines. Poor age constraints promote ambiguity among operators when discussing the formation.

To reduce the uncertainty surrounding the age, samples from three wells were submitted to Gerald Waanders (consulting Palynologist) for analysis. Cuttings were collected from the Fasken Fee BM # 1 SWD, Fasken Fee BL#1 SWD, and the Amoco David Fasken BS #1 wells. The BM and BS wells cuttings were compiled into 50 feet (15 meters) increments, while the BL well had sample intervals of 60 feet (18 meters). The occurrences of assemblages were paired with tops picked from logs. For the Amoco David Fasken BS #1 well, open hole logs were only available through the U.B.2 formation and the remaining tops were picked from the mud log. The results reveal that the Mississippian section in the study area encompasses the Chesterian, Meramecian, Osagean, and possibly the Kinderhookian stages (Figs. 15, 16 and 17, Appendix 1).

42-003-4216900



**FASKEN
BM #1 SWD**

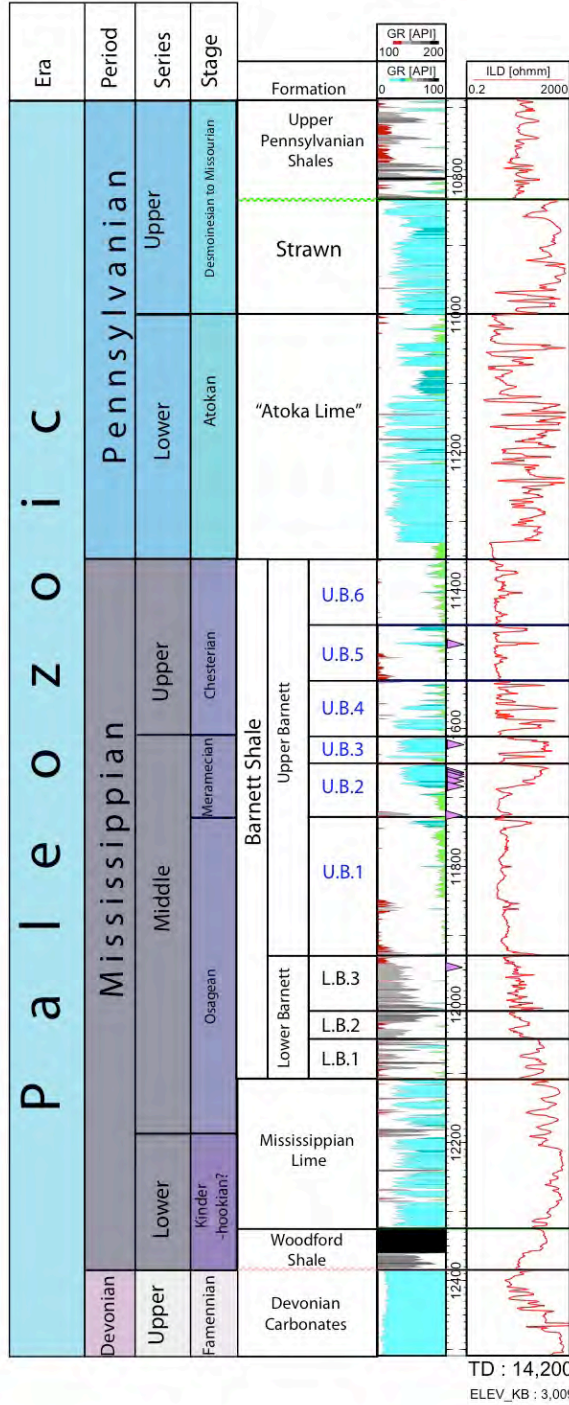


Figure 15. Palynology results tied into the Fasken Fee BM #1 SWD well.

42-135-41347



Fasken
BL #1 SWD

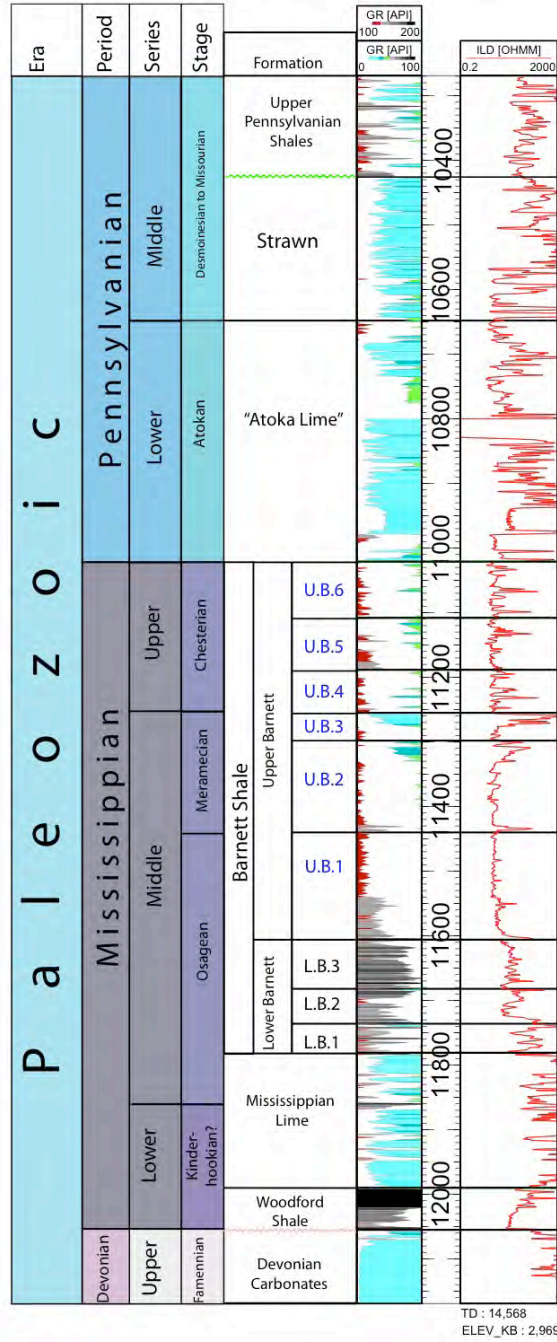
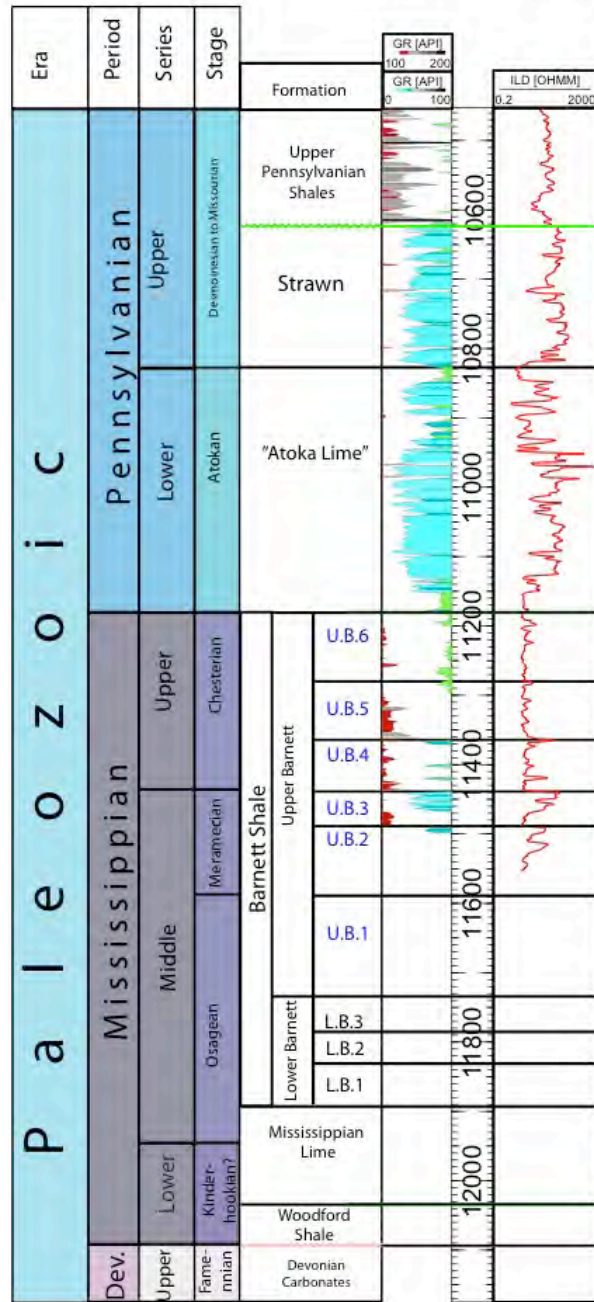


Figure 16. Palynology results tied into the Fasken Fee BL #1 SWD well.

42-329-3106500



AMOCO
David Fasken BS #1



TD : 13,850

ELEV_KB : 2,875

Figure 17. Palynology results tied into the Amoco David Fasken BS #1 well.

The top of the U.B.6 was found to be conformable with the first occurrences of Chesterian spores present in all three wells. The top of the Meramecian coincided with the top U.B.3 to the base of the U.B.2. Osagean assemblages of spores were first recorded around the shale marker denoting the top of the U.B.1 and encompass the entirety of the U.B.1, lower Barnett section, and the upper portion of the Mississippian Lime. Due to possible uphole contamination of samples, a tentative Kinderhookian age was assigned to the basal portion of the Mississippian Lime and the entirety of the Woodford Shale.

Sediment Accumulation

Isopach maps and cross sections show the patterns of sediment distribution and accumulation. Thickness presented on maps and cross sections portray the thickness of units following compaction. The Mississippian section ranges in thickness from approximately 980 feet (300 meters) in the northwest to 720 feet (220 meters) in the southeast (Fig. 18). Noticeable thinning of the section to 190 feet (60 meters) is observed at the McRae Farm #2 well drilled on an anticlinal structure in the southwestern region of the study area. The Mississippian Lime is thickest in the northwest, where it is 290 feet (90 meters) thick (Fig. 19). Thickness decreases to approximately 80 feet (25 meters) in the southeast. This thinning can be readily seen on cross sections along depositional dip (Fig. 20). Thickness of the lower Barnett varies from 210 feet (65 meters) to 136 feet (20 meters) (Fig. 21). However, a gross isopach map for the entire lower Barnett interval depicts thickness decreasing to the east, suggesting that a major depocenter was located to the west.

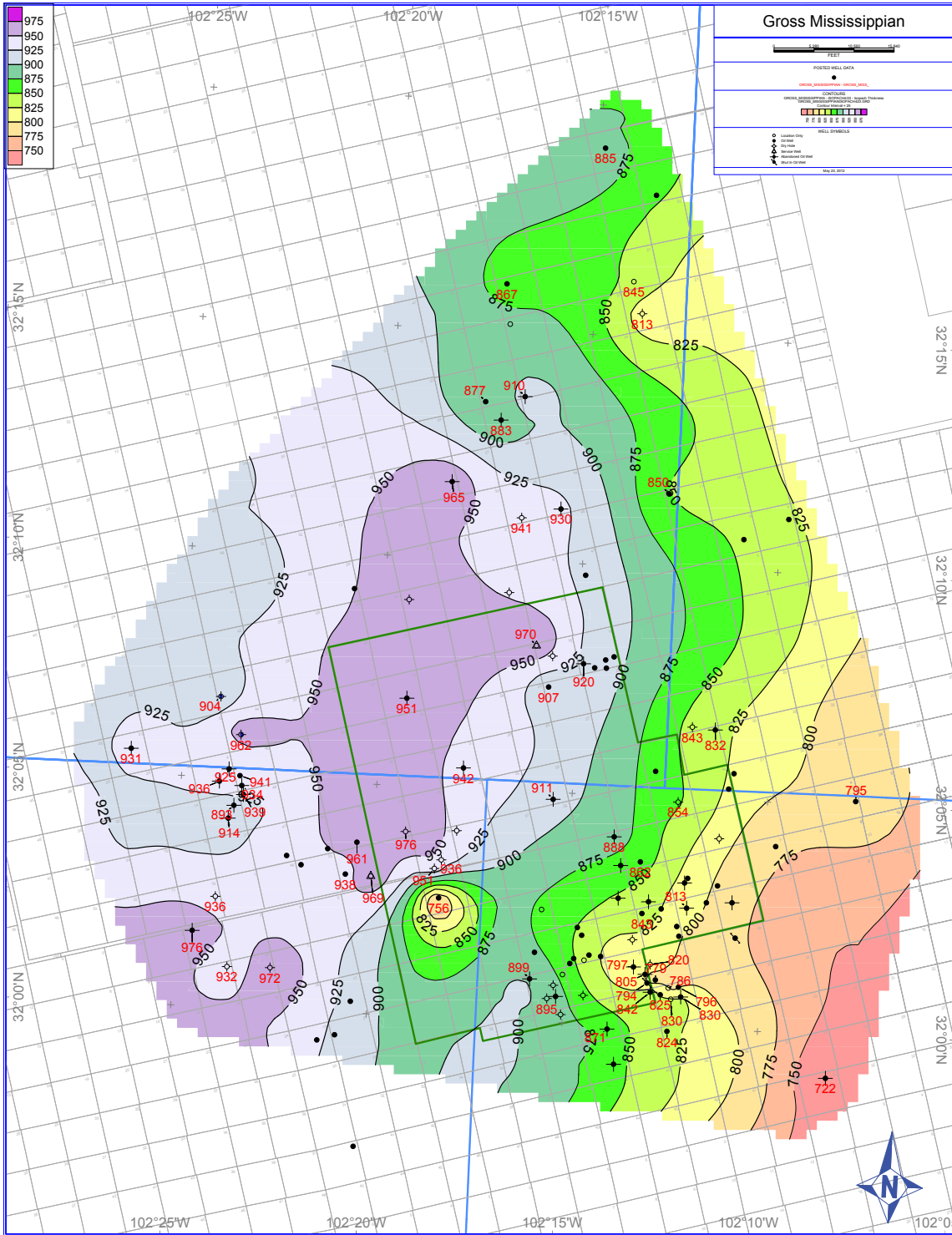


Figure 18. Gross isopach map for the entire Mississippian section. The overall westward thickening, and the thinning over the McRae farm #2 well are readily apparent. Contour interval is 25 ft.

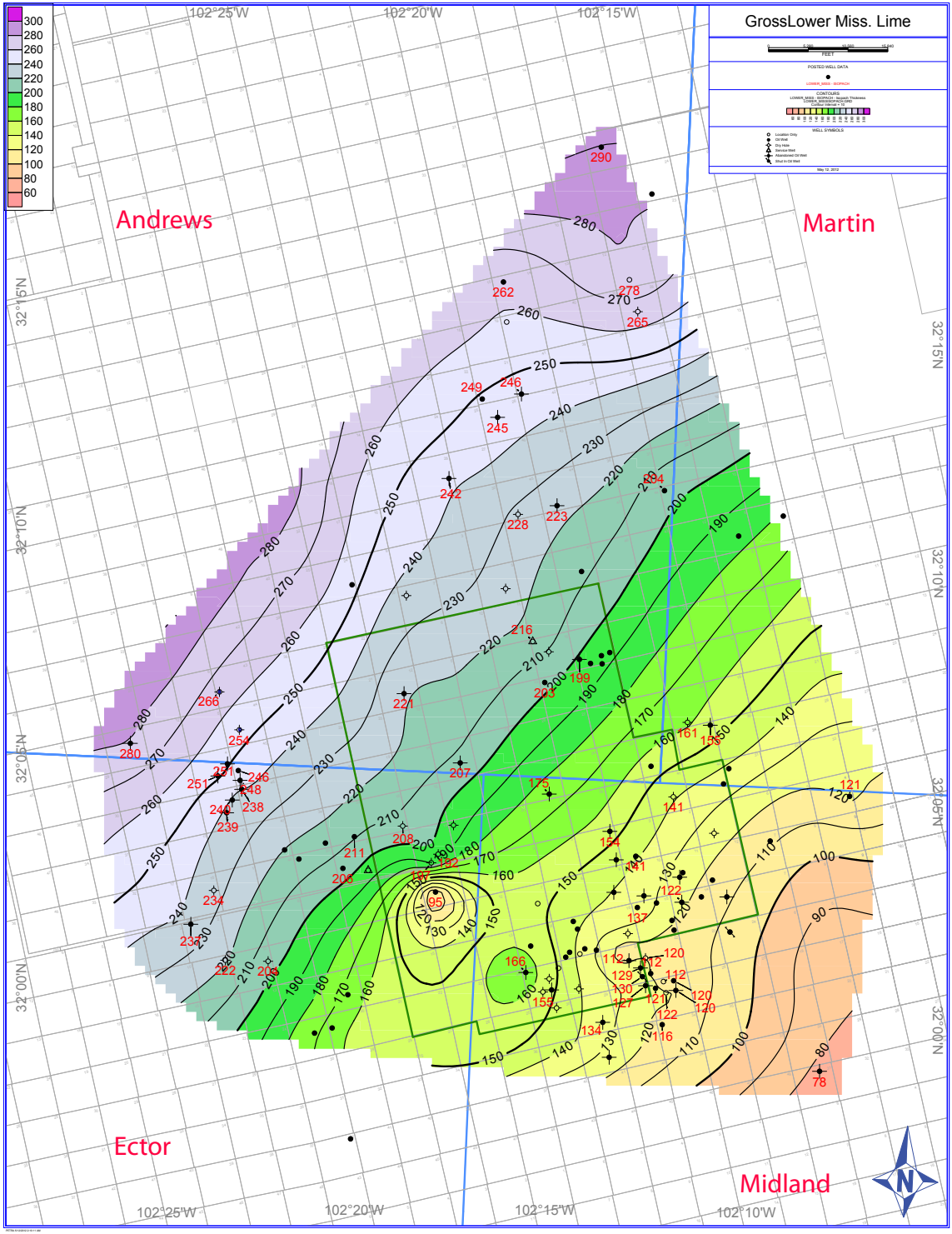


Figure 19. Gross isopach map for the Mississippian Lime. Notice the overall southeastward thinning, which likely reflects the southward dipping shelf. Contour interval is 10 ft.

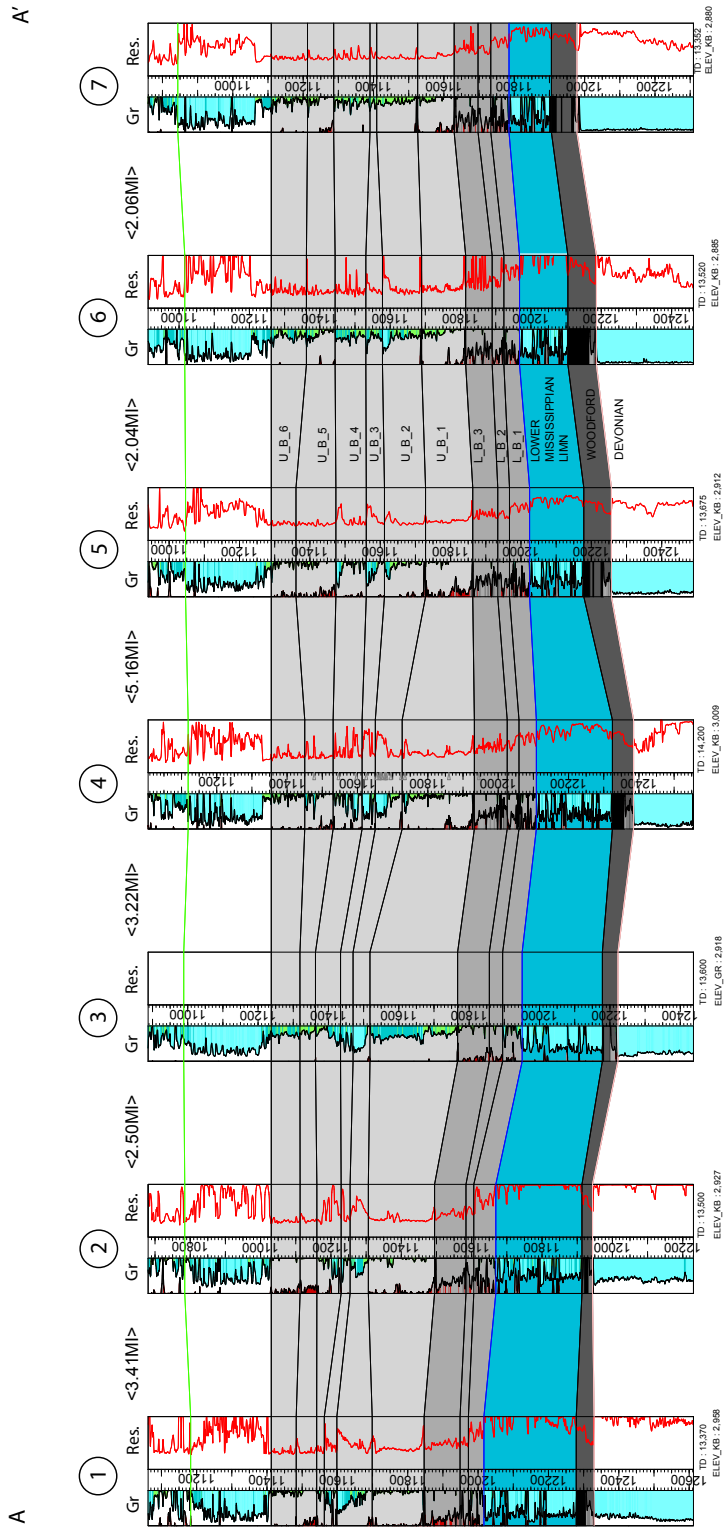


Figure 20. Stratigraphic cross section A-A' along depositional dip, flattened on the U.B. 6 shows the overall decrease in Mississippian lime thickness with dip. See Figure 3 for location of the section.

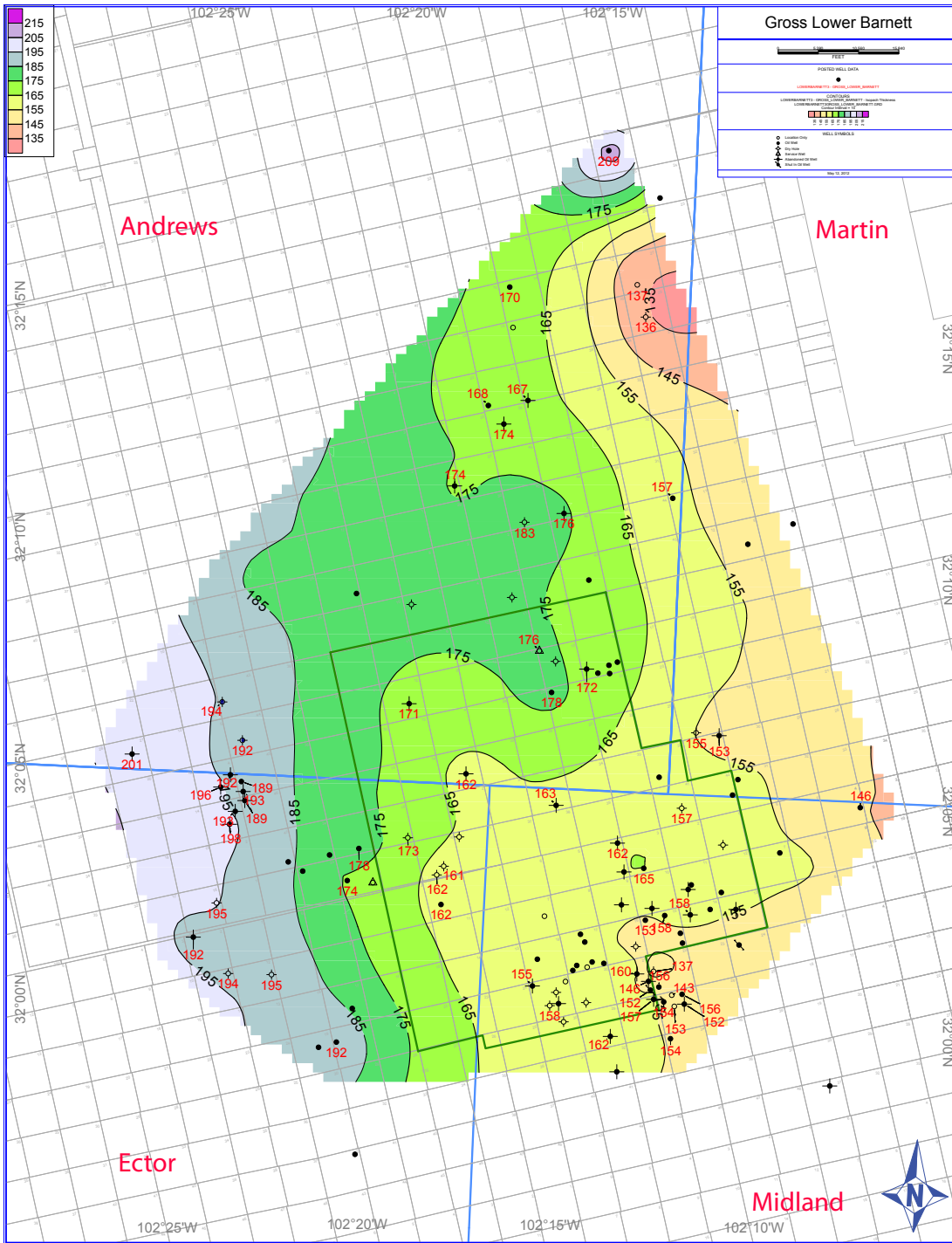


Figure 21. Gross isopach map constructed on the lower Barnett. The map shows a westward thickening. Contour interval is 10 ft.

To differentiate between basinal, siliciclastic-rich, shale and bioclastic debris flow strata in the upper Barnett, a cutoff of 14 Ωm is applied to the deep resistivity log (Fig. 22). Anything reading greater than 14 Ωm is taken to be representative of the more permeable debris flow units, and anything less is considered “tighter” shale. It should be noted, that a gamma ray cutoff would have been preferred, but due to various vintages of gamma ray curves, displaying a wide range of values for the cleaner sections, a gamma ray cutoff is misrepresentative of the debris flow section. A gross isopach map for the upper Barnett section shows thickness increasing north to south (Fig. 23), suggesting that the basin depocenter has slightly migrated to the south when compared with the underlying lower Barnett. When the cutoff of greater than 14 Ωm is applied to the section, a striking contrast is observed. With that cutoff, the section decreases from north to south (Fig. 24), suggesting a northern source for the upper Barnett carbonate debris. Cross sections along depositional strike also show an overall decrease towards the south in the electrofacies representative of the carbonate debris (Fig. 25 and 26). Since established production has been achieved from the U.B.2 bioclastic debris (see below), gross and net isopach maps were also constructed for the U.B.2 (Fig. 27 and 28). Similar patterns to the gross and net isopach maps for the upper Barnett emerge for the U.B.2. While the gross isopach map for U.B.2 shows thickening to the south, the net isopach map again shows a thick in the north and thin in the south. The pattern of the net isopach maps suggests a northern source for the mass gravity flows.

42-003-42169



**FASKEN
1 SWD**

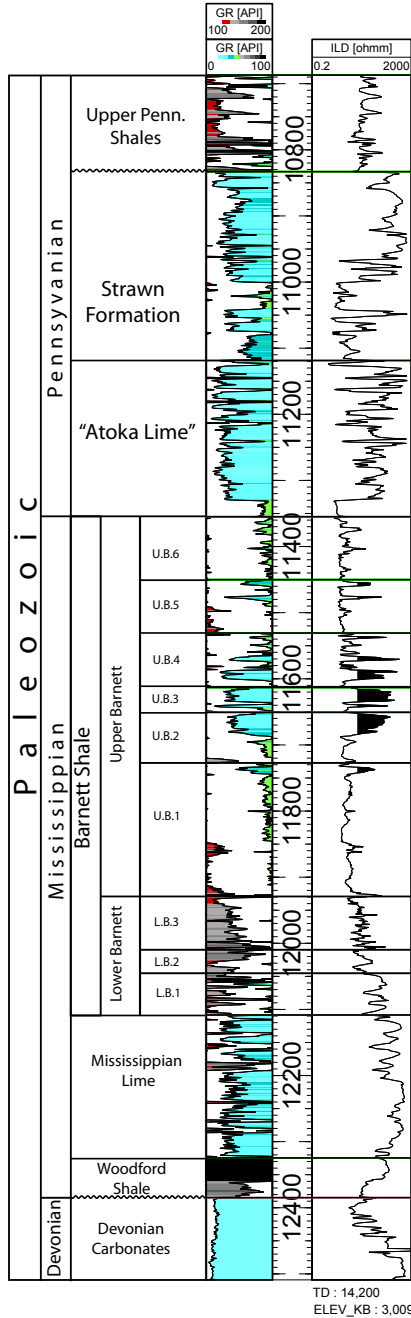


Figure 22. Type log showing the $>14 \Omega\text{m}$ cutoff used to differentiate between shales and bioclastic debris flows. Shaded areas coincide with $>14 \Omega\text{m}$.

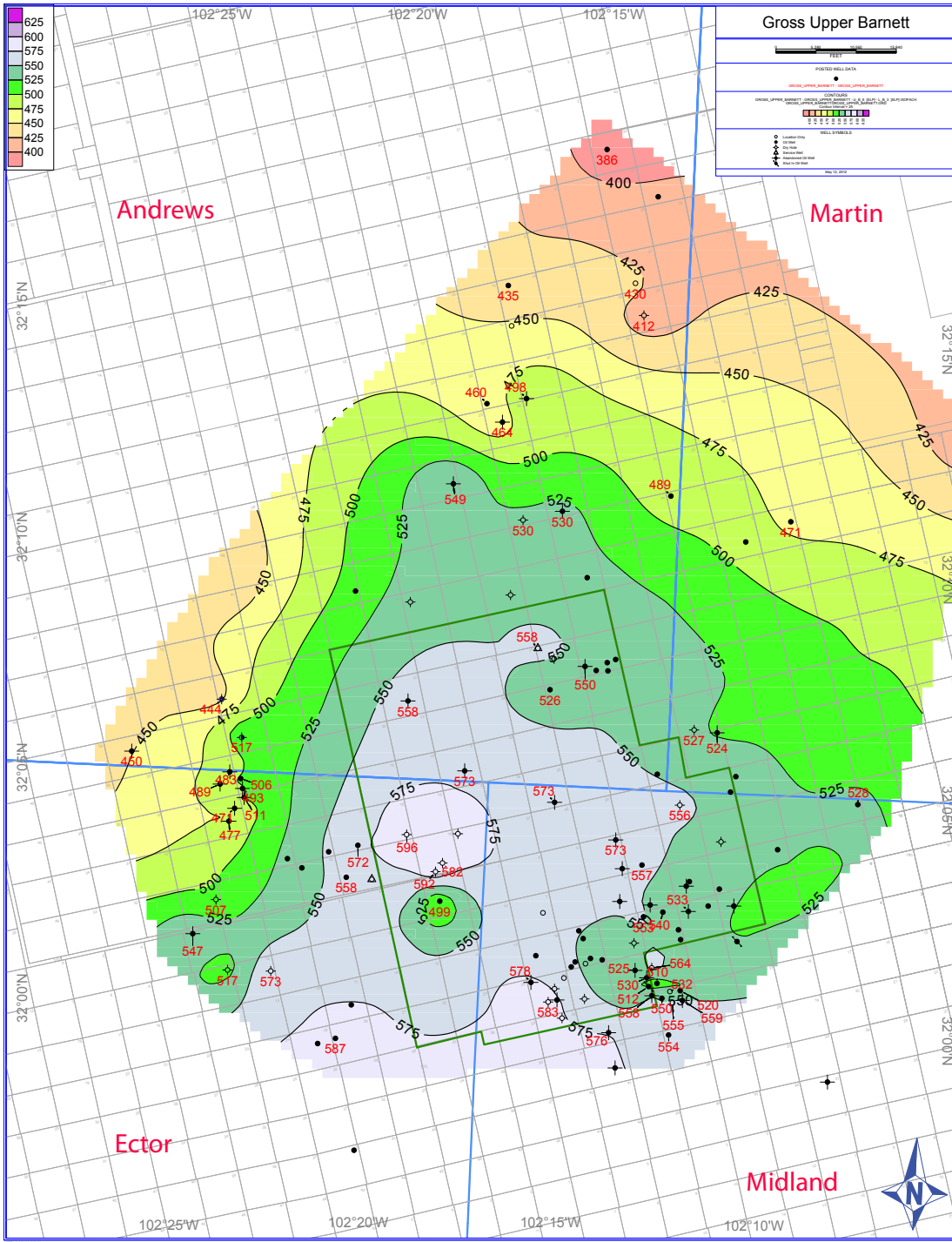


Figure 23. Gross isopach map for the upper Barnett. The map pattern suggests that the main depocenter has shifted slightly towards the south since the deposition of the lower Barnett. Contour interval is 25 ft.

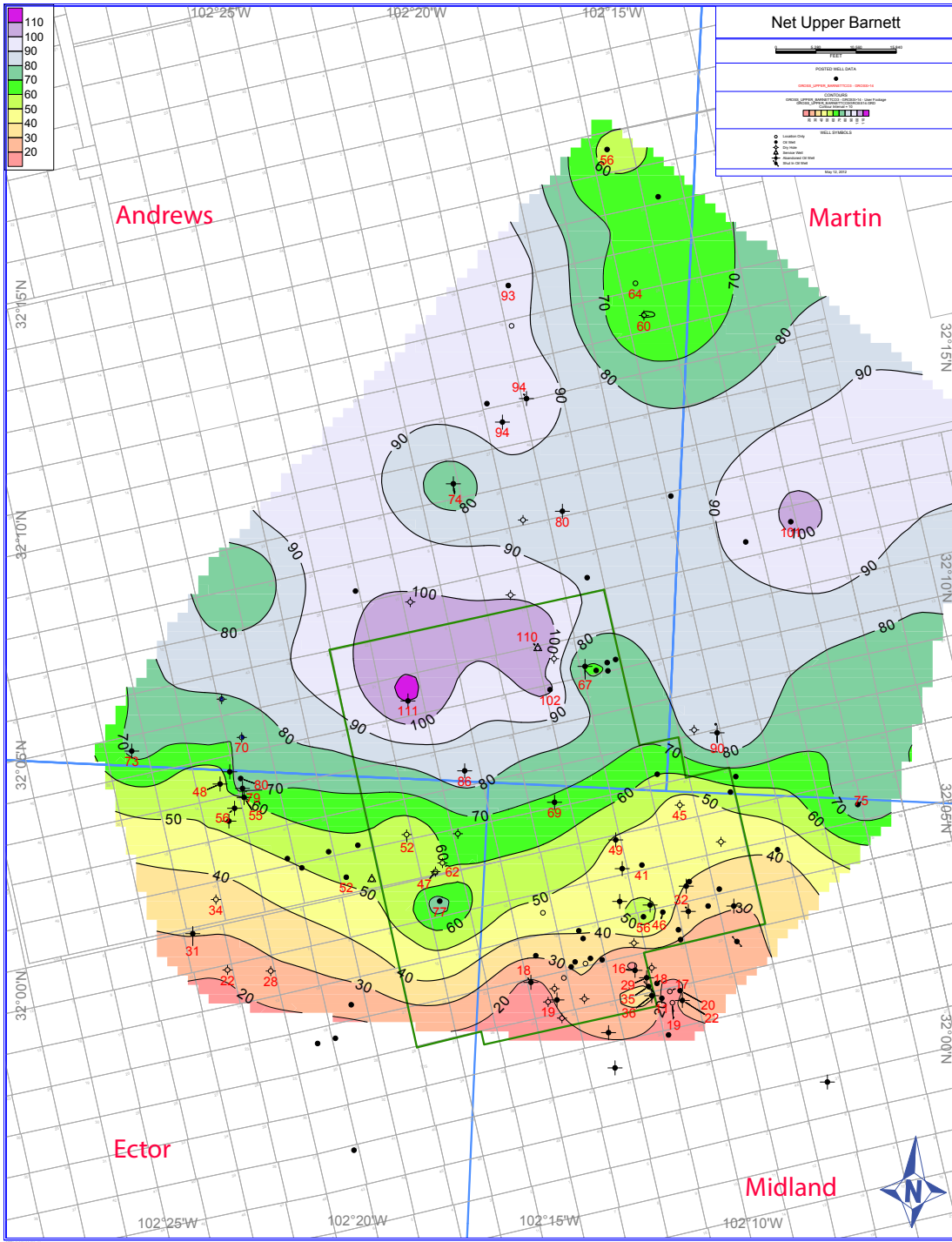


Figure 24. Net isopach map for the upper Barnett showing a southward thinning of strata. Contour interval is 10 ft.

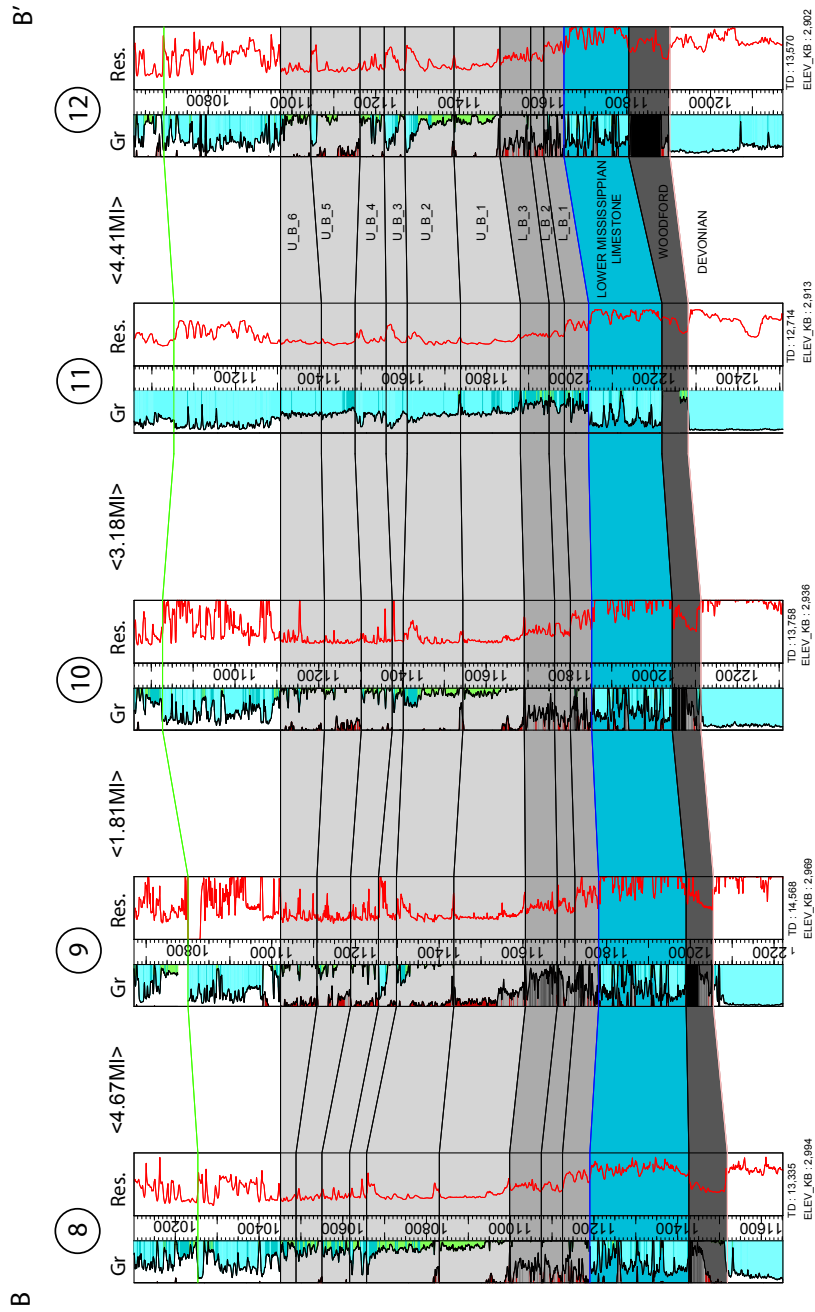


Figure 25. Stratigraphic cross section B-B', flattened on the top of the U.B.6, along depositional strike. Notice the overall thickness of the U.B.2 clean GR electrofacies. For location of the section see Figure 3.

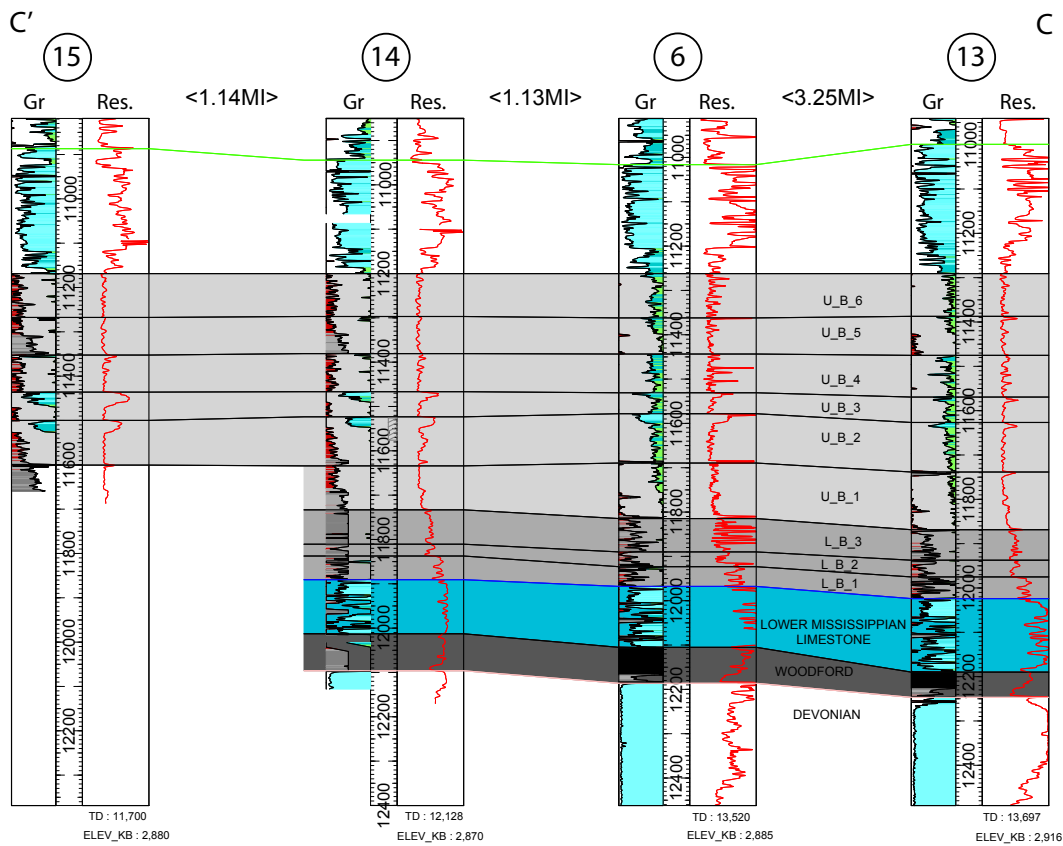


Figure 26. Stratigraphic cross section C-C', flattened on the U.B.6, along depositional strike showing an overall decrease in the clean GR sections for the U.B.2, which represents the bioclastic debris flows, when compared to cross section B-B' located to the north. For location of the cross section see Figure 3.

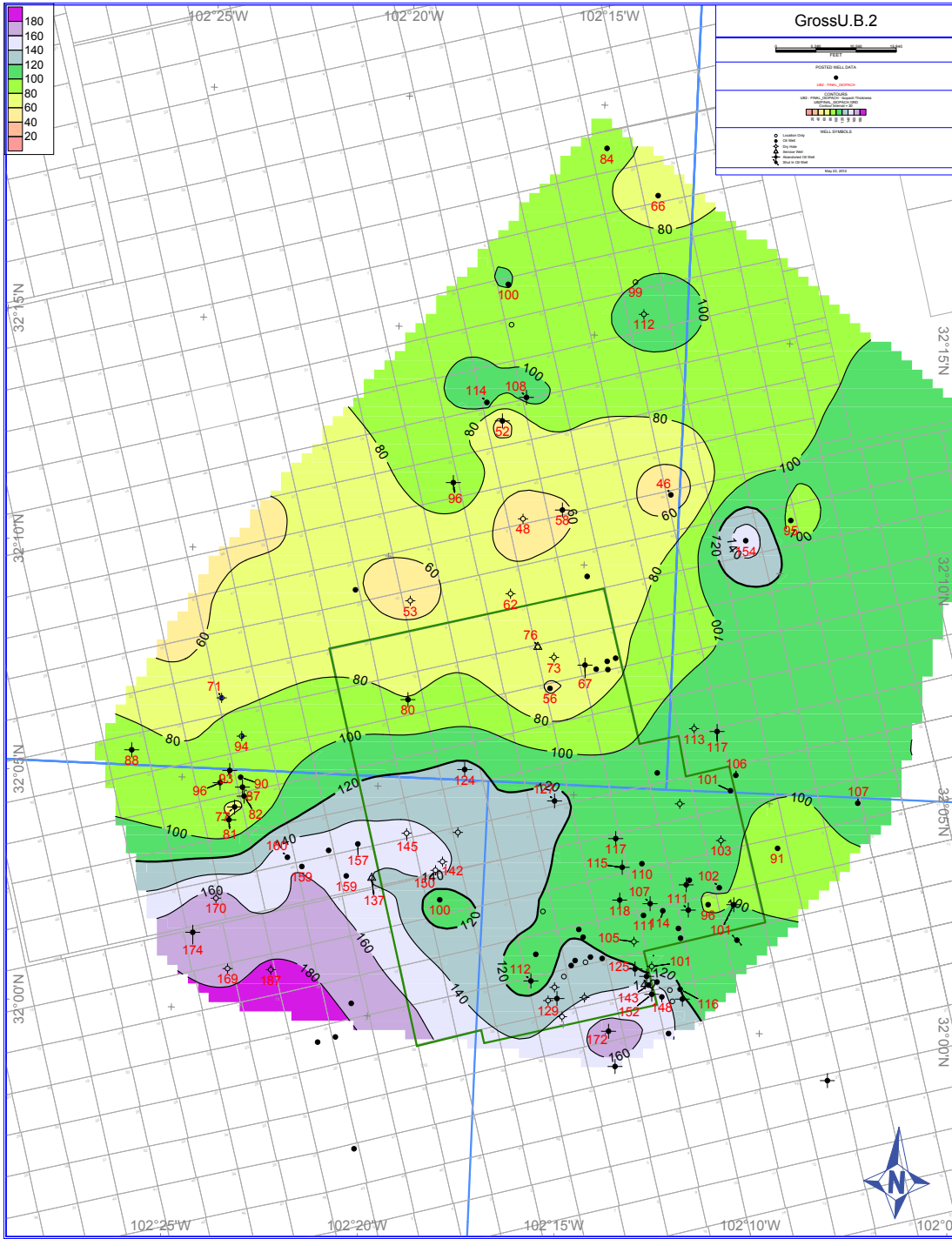


Figure 27. Gross isopach map for the U.B.2 showing a northwestward thinning. Contour interval is 20 ft.

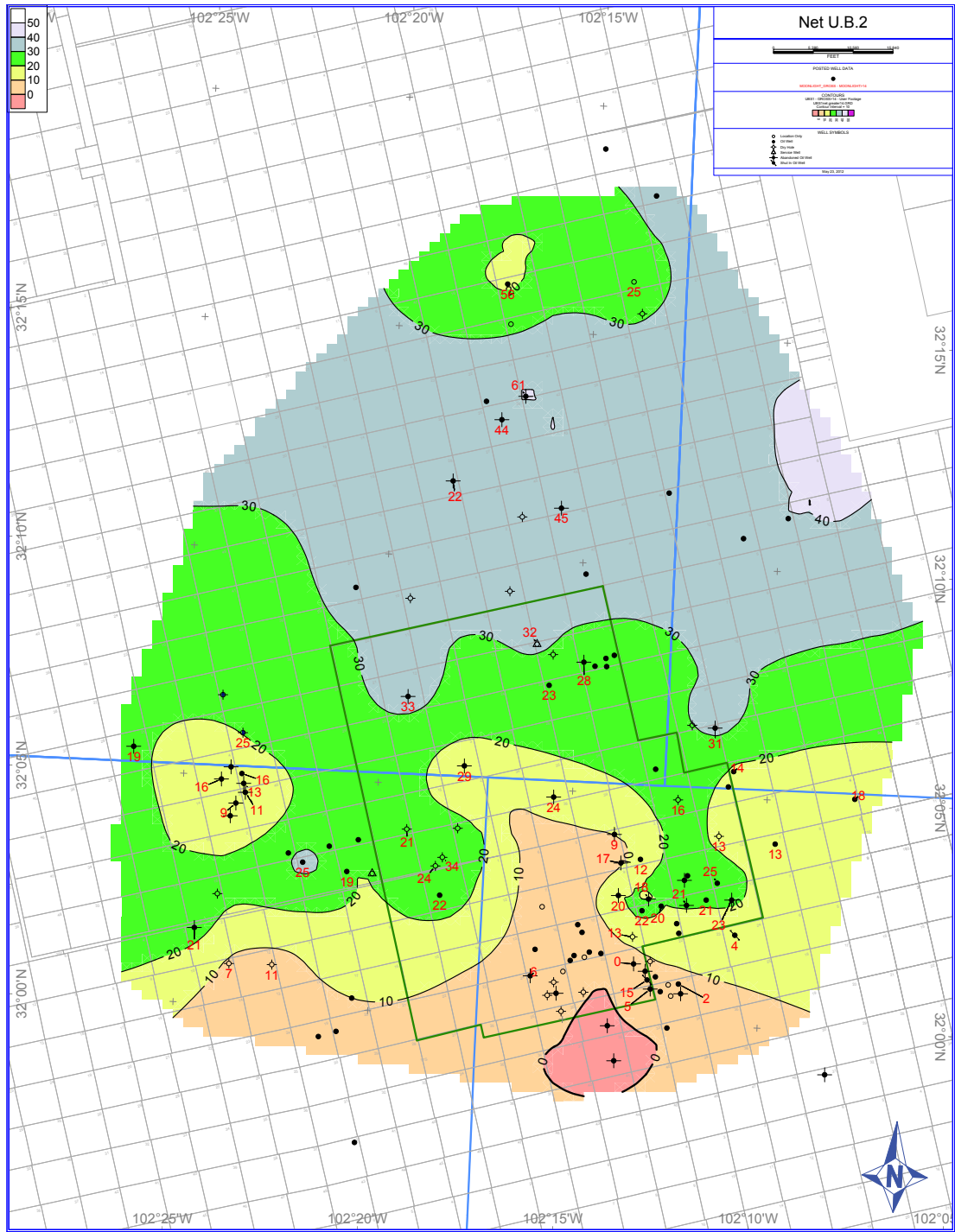


Figure 28. Net isopach map constructed for the U.B.2 showing a southward thinning. Contour interval is 10 ft.

Regional Context

Carbonates sourced from a platform in the north and shale deposited in a basin in the south characterizes the two distinct lithologies present in Mississippian strata (Ruppel and Kane, 2006) (Fig. 29). Carbonates were deposited up dip on a southwest- to west-dipping shelf grading into deeper water limestone, progressively thinning basinward into basinal shale that comprises the Barnett Shale Formation. The southernmost extent of the carbonate platform is located north of the study area in Gaines and northern Andrews Counties (Bay, 1954). The shelf has been eroded over the Central Basin Platform, but remains present in central Lea County, New Mexico (Hamilton and Asquith, 2000). Elsewhere in the basin, hemipelagic sedimentation dominated resulting in the formation of siliceous shale. Maximum thickness of shale is recorded in portions of Reeves and Ward County (Craig and Conner, 1979; Wright, 1979). The positive features of the Diablo uplift and Pedernal Massif defined the southern and western limits of the basin (Fig. 29) and provided the bulk of the siliciclastic sediment to the basin. Starting around the mid-late Mississippian, uplifted portions of the advancing Ouachita trough also served to provide siliciclastic input in the southern regions of the basin (Ruppel and Kane, 2006).

Existing isopach maps for the Mississippian in the Permian Basin show a major depocenter roughly corresponding to the locality of the ancestral Central Basin Platform with strata thinning eastward (Fig. 29; Wright, 1979). The study area falls just shy of the 1000 feet contour line on the isopach map for Mississippian strata. Observed thickness in the study for gross Mississippian strata is 975 feet (300 meters). The eastward thinning is also reflected in the gross Mississippian isopach map for the study area.

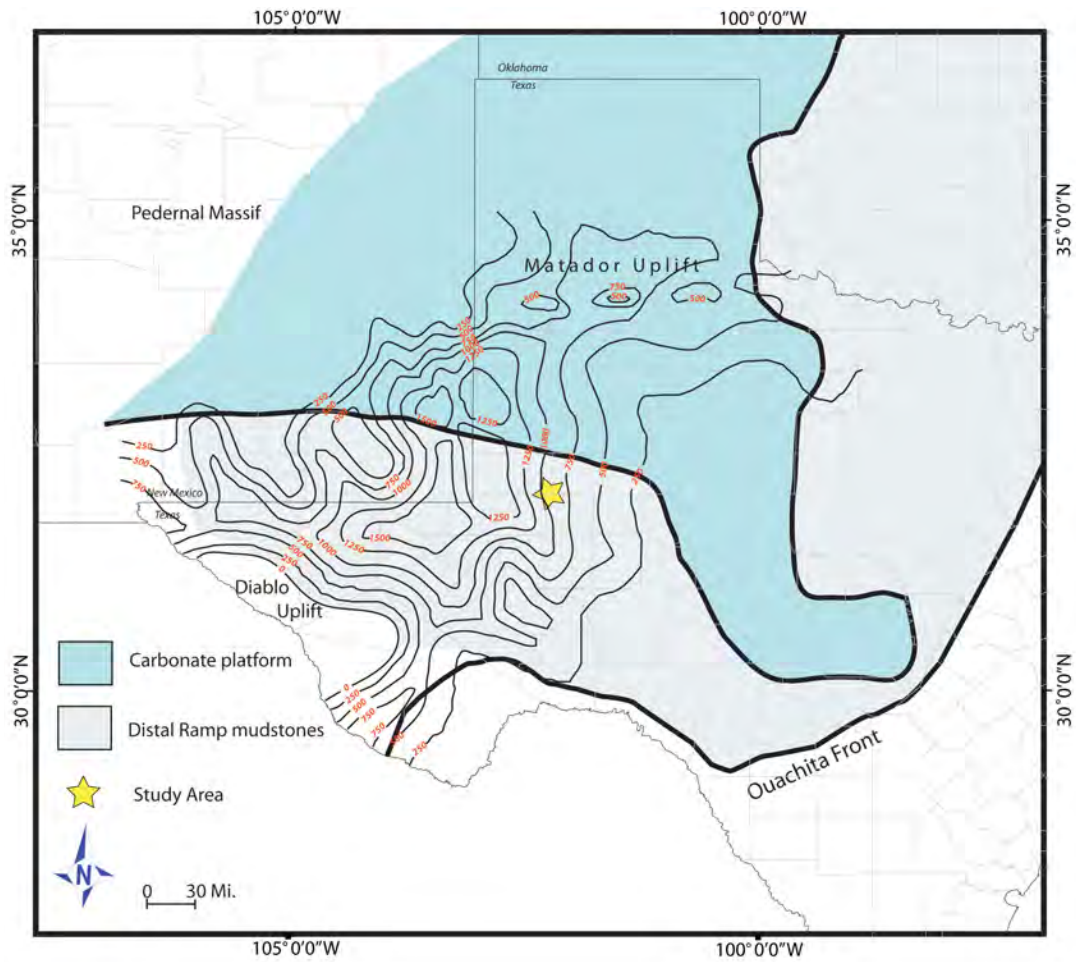


Figure 29. Paleogeographic map showing the Permian Basin region during the late Mississippian. Isopach map shows a major depocenter corresponding to the western portion of the study area (yellow star). Contour interval is 250 feet. Map is after Wright (1979) and Ruppel and Kane (2006).

Structure of Study Area

Accumulation of Mississippian sediment varied minimally from that of the Devonian, such that the major depocenters of the Tobosa Basin maintained their role (Wright, 1979). During the Late Mississippian, the Tobosa Basin was subjected to various structural changes, including the initial pulses of the Marathon-Ouachita orogeny. The emergence of the Central Basin Platform during this time resulted in the division of the Tobosa Basin into two separate depositional entities with the Delaware Basin to the west and the Midland Basin to the east. Regionally, the Midland Basin displays an asymmetric character, with the basin axis running approximately north-south, deepening to the west.

Regional dip is steepest in the west along the flanks of the Central Basin Platform and lessens to the east towards Martin County. Structure contour maps constructed on the top of the Woodford, the top of the L.B.3, the U.B.2, and U.B.6 all reflect the same overall geometry (Figs. 30-33). The measured depth to the top of the Mississippian section in the study area ranges from 9,000 feet (2,750 meters) in the west to 11,500 feet (3,500 meters) in the east. Locally, anticlinal and synclinal features are recognized in the southern portion of the study area. These are presumably a by-product of the structural regime changes associated with deformation along the flanks of the Central Basin Platform.

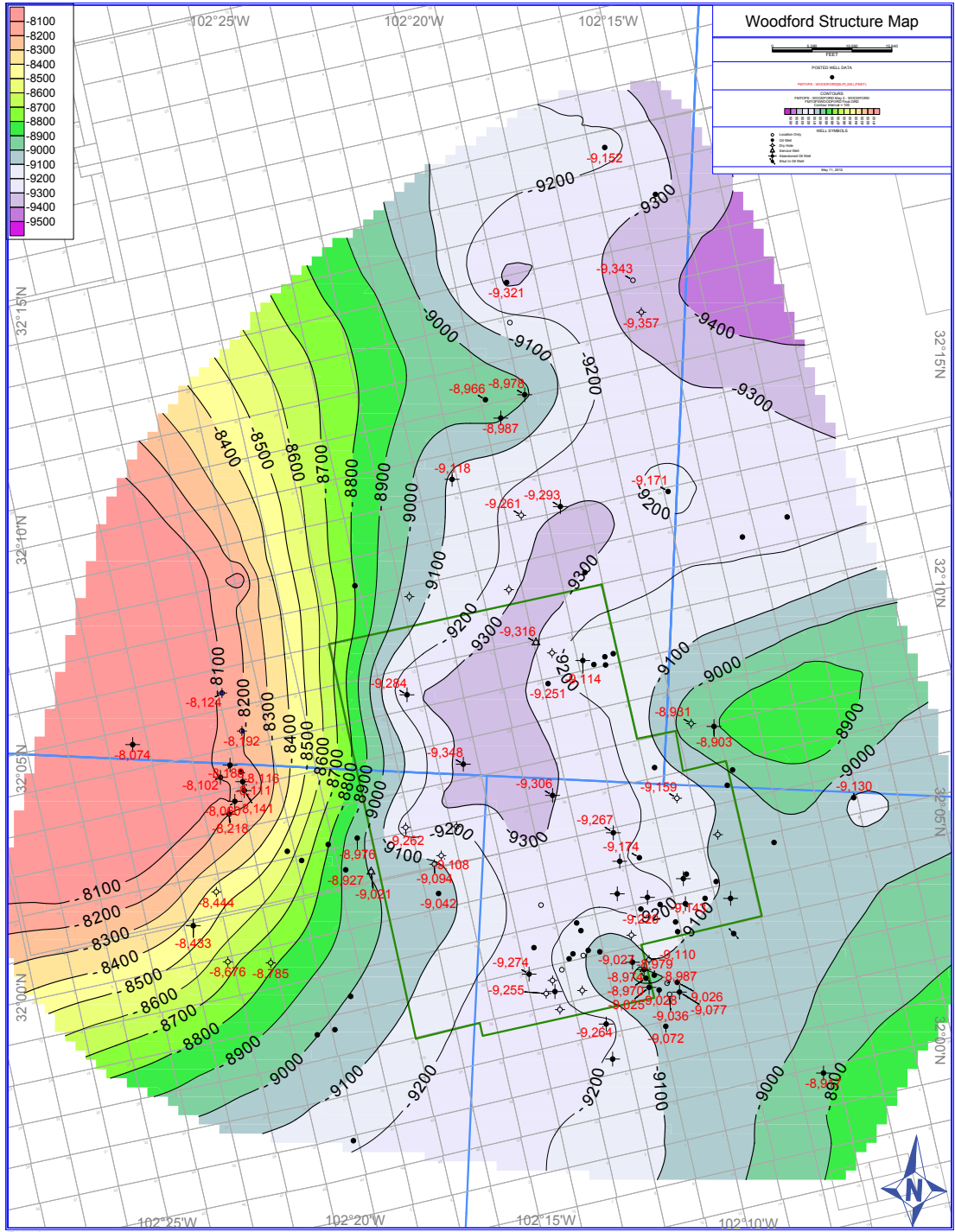


Figure 30. Structure contour map of the top of the Woodford Shale. The map depicts a post-depositional low that trends north-south throughout the central portion of the study area. Contour interval is 100 ft.

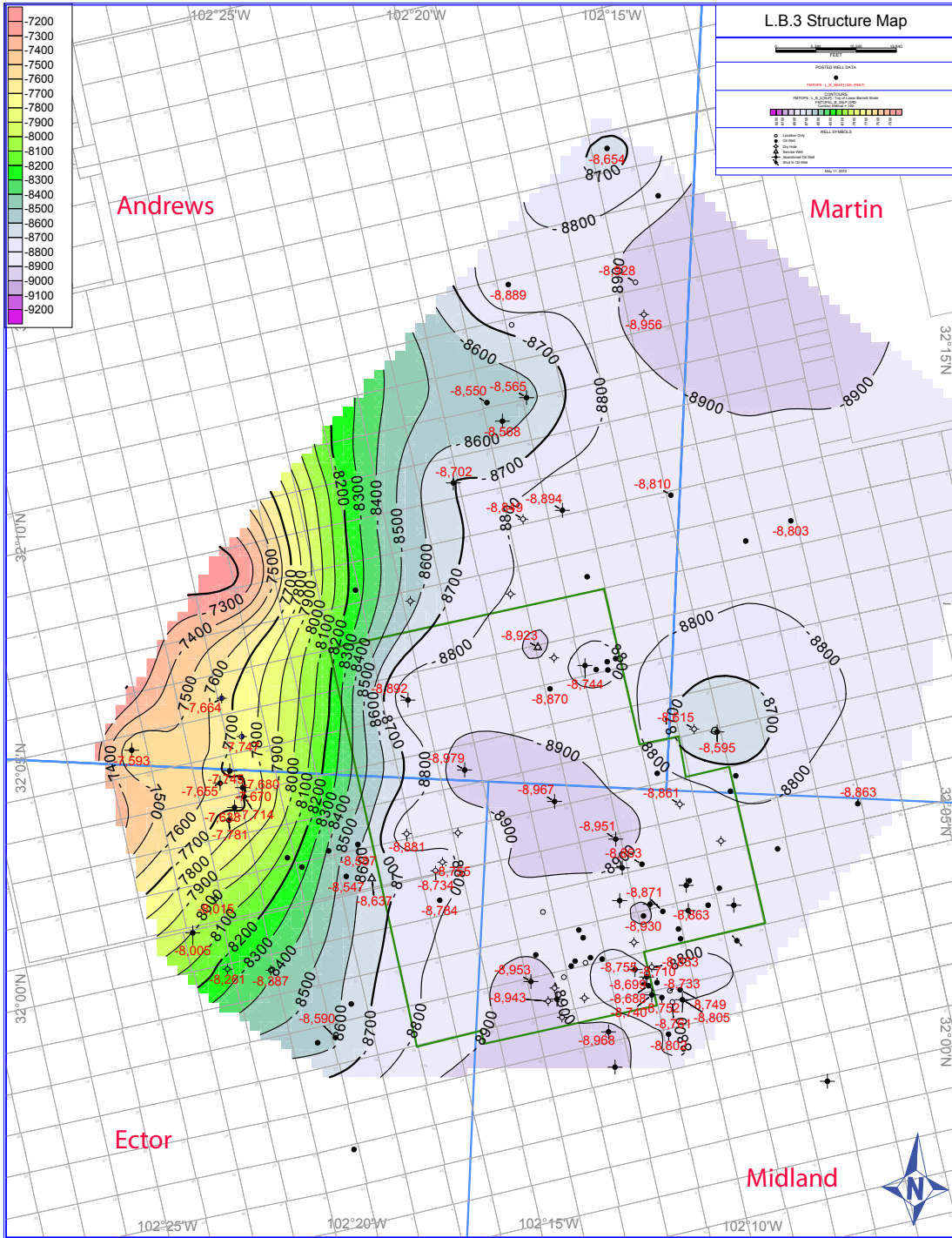


Figure 31. Structure contour map of the top of the L.B.3. Folds are present in the eastern and southeastern portion of the area. Contour interval is 100 ft.

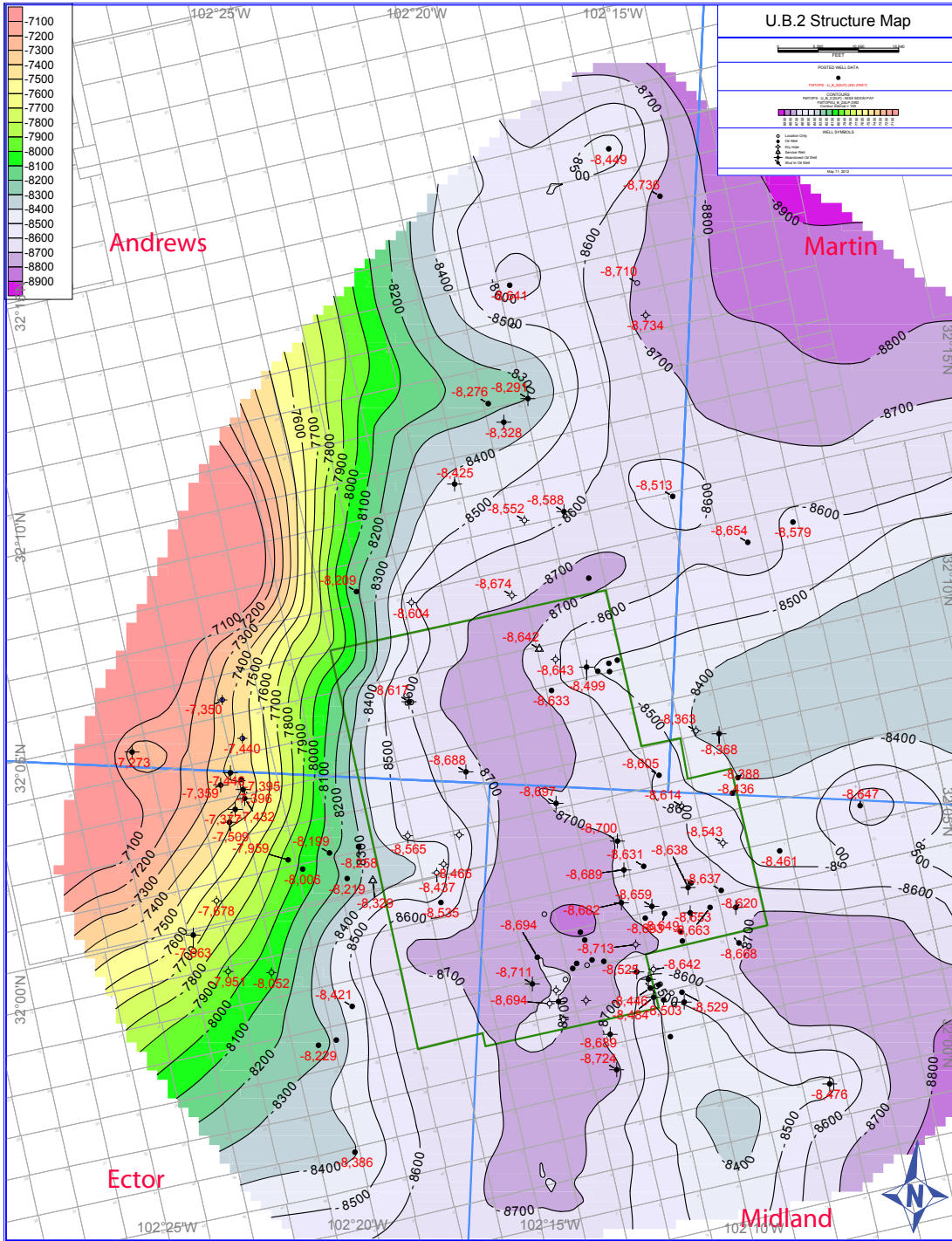


Figure 32. Structure contour map atop of the U.B.2 subdivision. Overall geometry is similar to the preceding maps. Contour interval is 100 feet.

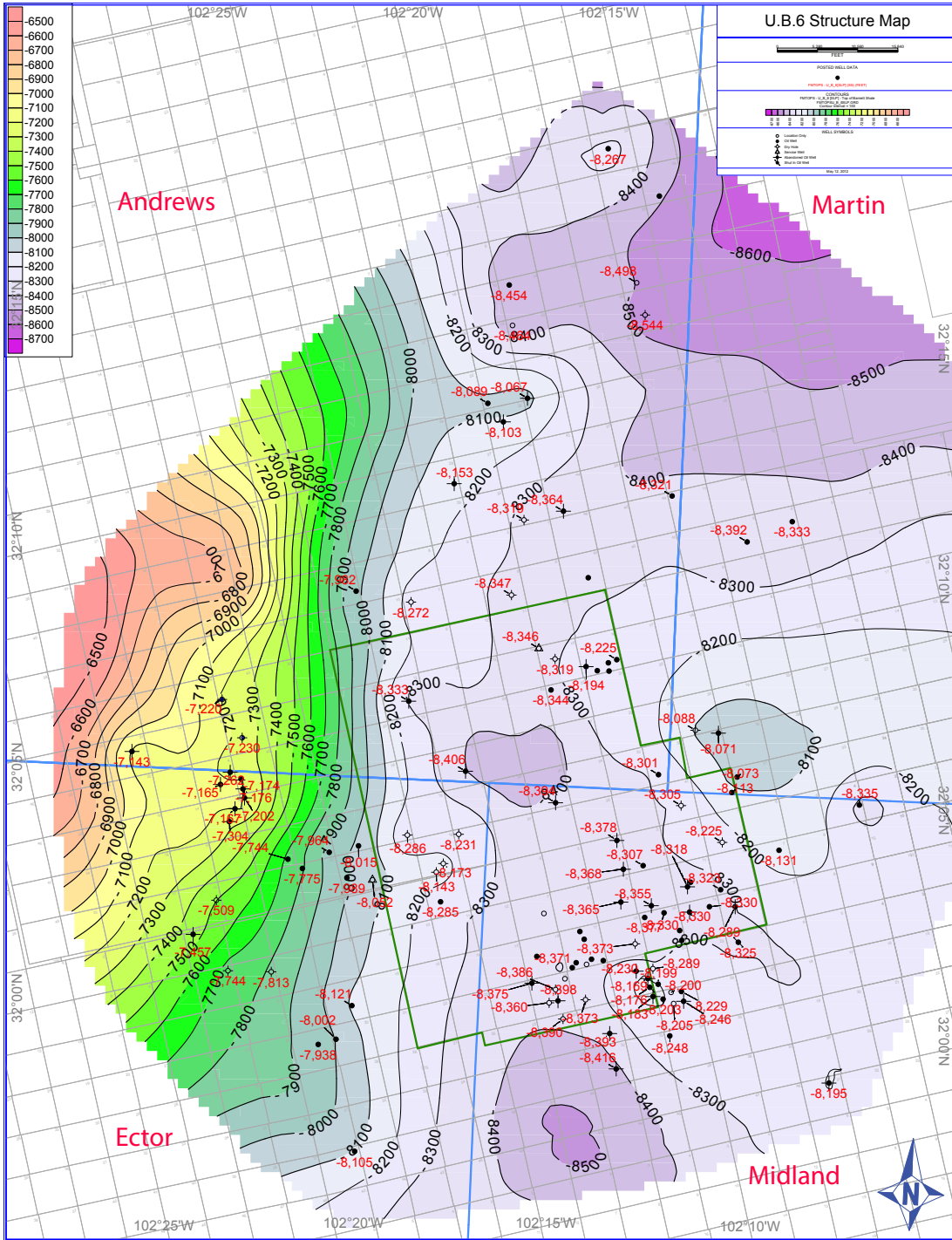


Figure 33. Structure contour map of the top of the U.B.6 subdivision. Various folds are present in the eastern part of the study area. Contour interval is 100 ft.

Discussion

Strata comprising the lower Barnett were deposited in deep-water marine conditions. The sidewall core sample taken from the lower Barnett interval, coupled with the overall elevated gamma ray responses for the entire interval suggest hemipelagic sedimentation exerted strong influence on the accumulation of strata. This is further suggested by the dearth of terrigenous constituents present in the sample (Table 2). The high TOC content is a by-product of anoxic conditions persisting throughout deposition, which also resulted in the formation of pyrite. The thickest accumulations of the lower Barnett coincide with the present-day location of the Central Basin Platform. High S1 and S2 values from the lower Barnett sample reveals that the interval contains sufficient properties to have generated hydrocarbons.

The upper Barnett is composed of both calcareous/phosphatic shale and silty limestones deposited in marine conditions. The presence of phosphate nodules and pyrite framboids suggest an anoxic environment. The high density of pyrite and phosphate could potentially affect any density measurements throughout the section.

A gross isopach of the entire upper Barnett section shows the thickest section in the southeast. This pattern suggests that the main depocenter shifted slightly to the south following the deposition of the lower Barnett. This shift may reflect early subsidence related to the emergence of the Central Basin Platform (Fig. 23). The net isopach map, taken to represent deposition of bioclastic debris, shows the thickest portion in the north, decreasing in overall thickness to the south. This pattern is opposite to the gross isopach pattern and suggests a northerly source for the flows. The likely source is the carbonate

platform that was present north of the study area during the Chesterian. If this is correct, the carbonate constituents that comprise the debris flows were likely episodically sourced from the platform to the basin via mass-gravity flows (Fig. 34).

Production History

Upper Mississippian fields in the Midland Basin are located in both platform and basin environments. On the platform, trapping mechanisms are either structural or stratigraphic, with limestone, dolomite, and/or chert providing the reservoir (Wright, 1979). South of the paleo-platform, fields including Moonlight, Lowe, Desperado, and Bradford Ranch produce from the bioclastic-rich debris flows present in the upper Barnett (Fig. 35). Not all fields are reported Mississippian, although that may be a consequence of the aforementioned lack of age consensus. The trapping mechanism is stratigraphic, which is a result of the detrital units thinning out on the flanks of the sequence. A fracture network likely provides the means of production viability from the “tight”, low porosity, low permeability reservoirs. Evidence for this includes a well’s ability to drain an entire section and the abnormal pressure gradients (Unpublished Field Reports). One example of the abnormal pressure gradient is a pressure test that was applied to the Moonlight field. The test consisted of shutting in wells producing from upper Mississippian units, while a new one was brought online. Wells 8,500 feet (2,590 meters) away recorded a pressure drop in an hour (Jim Henry, Petroleum Engineer, personal communication, 2012). Well communication in that short time frame strongly suggests the presence of a fracture network. Additionally, core recovered from the Fasken 215-B in the Moonlight Field has a five-inch fracture from the U.B.2 bioclastic

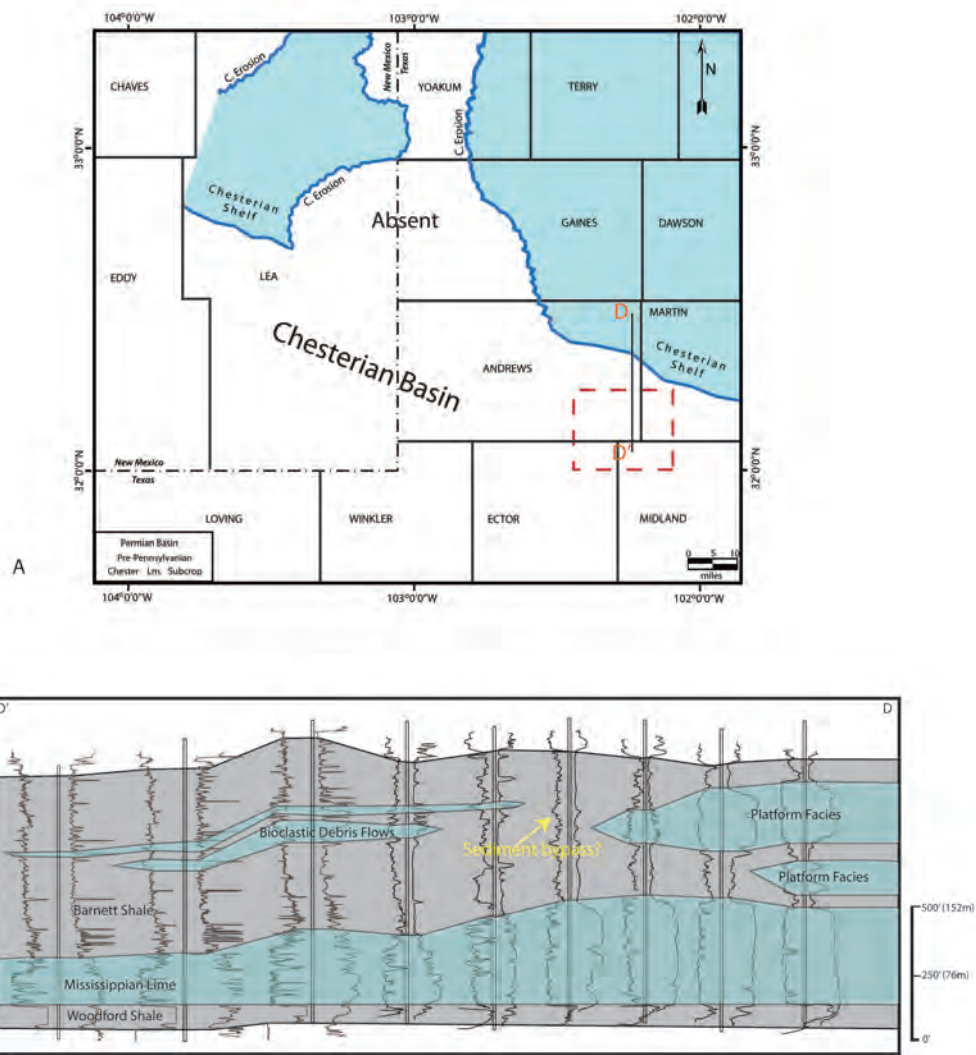


Figure 34. A) Location of cross section D-D' in relation to the study area (dashed red rectangle) and the Chesterian shelf. Modified from Hamilton and Asquith (2000). B) Idealized integration of the deposition of bioclastic mass-gravity flows in study area into Bay's (1954) cross section. Modified from Bay (1954) and Ruppel and Kane (2006).

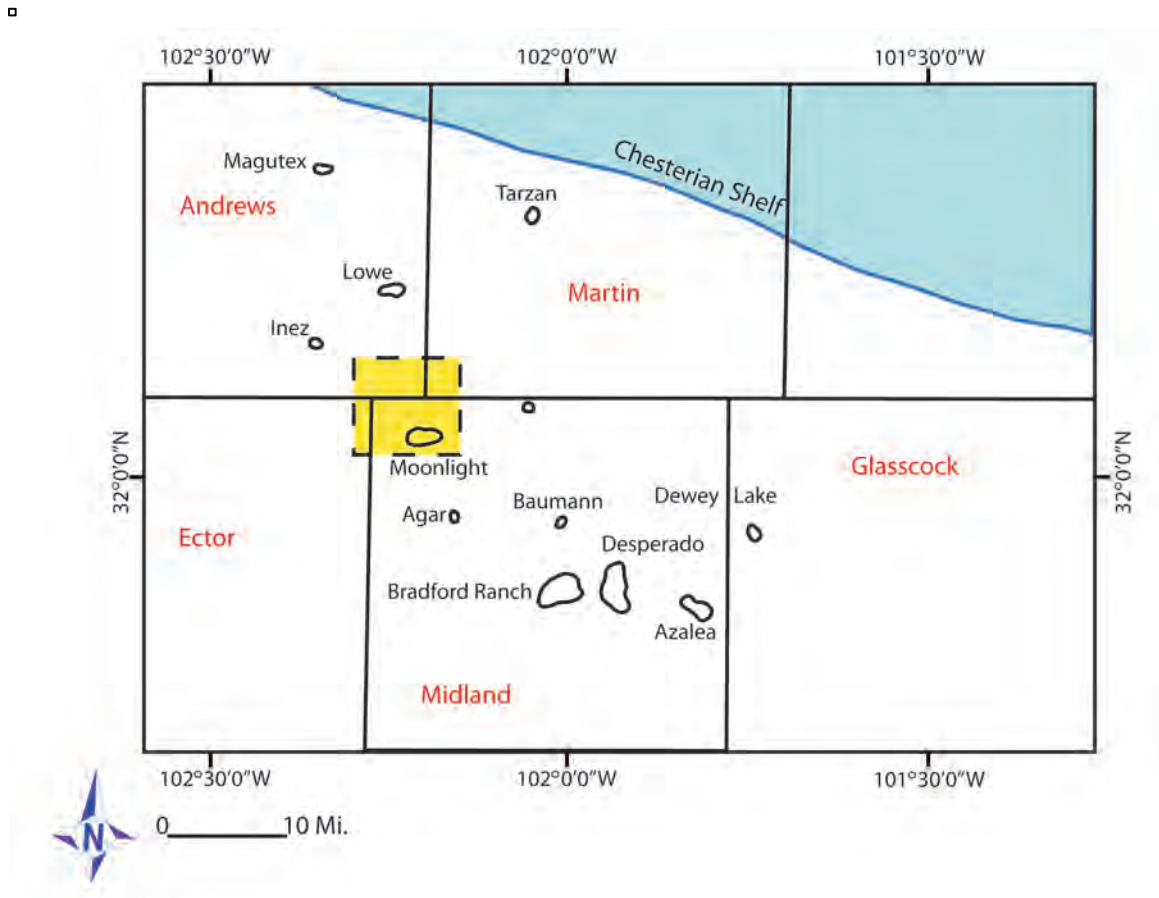


Figure 35. Map of oil fields that have produced hydrocarbons from the upper Barnett. Study area highlighted in yellow. Modified from Anonymous (1986).

carbonate section (Al Smith, Independent Geologist, personal communication, 2011). Upper Mississippian detrital units were actively pursued in the mid seventies to late eighties until an unfavorable economic climate curtailed activity.

Favorable economic prices have once again shifted focus to the liquids-rich Midland Basin, with the “Wolfberry” (Permian) play dominating the industry’s focus. Wolfberry trends overlap areas that were mapped containing thick portions of the upper Barnett detritus strata. While it would increase well costs to drill deeper and test, the potential for increased pay warrants exploration. All of the wells drilled in the original fields were vertical. With the increased expertise of horizontal drilling, the ability to increase contact to the “tight” reservoir coupled with fracture stimulation completion, could aid in increasing permeability.

Conclusions and Recommendations

The top of the shale sequence underlying the “Atoka Lime” is presumptively Chesterian in age, making it equivalent to the Barnett Shale Formation. Depths to the top of the Barnett section range from ranges from 9,000 feet (2,750 meters) in the west along the flank of the Central Basin Platform to 11,500 feet (3,500 meters) in the east. It can be divided into an upper, calcareous unit and a lower, siliceous unit on the basis of resistivity and GR responses. The upper unit can be further subdivided into six subunits by log responses, to further aid in deciphering depositional trends. Isopach maps constructed on the subunits containing carbonate detritus gravity flows suggest a northern source, which coincides with the late Mississippian platform margin. Future work in

delineating the overall geometry and transport mechanics (point vs. line source) will be crucial to further understand the deposition patterns.

Historically, established production comes from the upper subunits containing increased porosity and permeability values. The encasing shales are likely to provide the source. Although fracture detection was not completed in this study, it is likely to exert significant control on the ability to exploit hydrocarbons. Preliminary analysis suggests that weight percent TOC values can be estimated from the amount of separation from GR and Rt curves. The lower Barnett had the highest TOC and gas shows, based on core and petrophysical analysis.

Future study of the Barnett in the Midland Basin should incorporate petrophysical, geophysical, geochemical, and core analysis. More age data should be gathered from palynology and conodonts to better constrain the sequence. With the benefit of being located in a mature province, old well logs and core reports are readily available and should be used to further carry out correlations. Azimuthal angle versus offset analysis and seismic coherency could provide the means to predict natural fracturing in the sequence, aiding in delineating specific trends that warrant exploration focus. While historic production has solely come from the upper subunits, the lower Barnett with its appreciable TOC, S1 and S2 values could prove to be a viable horizontal prospect.

References

- Adams, D.C., and Keller, G.R., 1996, Precambrian basement geology of the Permian Basin region of West Texas and Eastern New Mexico: A geophysical perspective: American Association of Petroleum Geologists Bulletin, v.80, p. 410-431.
- Adams, J.E., 1965, Stratigraphic-tectonic development of the Delaware Basin: American Association of Petroleum Geologists Bulletin, v. 49, p. 2140-2148.
- Adams, J.E., Frenzel, H.N., Rhodes, M.L., and Johnson, D.P., 1951, Starved Pennsylvanian Midland Basin: American Association of Petroleum Geologists Bulletin, v. 23, p. 1673-1681.
- Anonymous, 1986, Unraveling the mystery of the Atoka: Search, v. 2, p. 1-5.
- Ball, M., 1995, Permian Basin Province (044), *in* Gautier, D.L., Dolton, G.I. Takahashi, K.T., and Varnes, K.L., eds., 1995 National assessment of United States oil and gas resources-Results, methodology, and supporting data: U.S. Geological Survey Digital Data Series DDS-30.
- Bay, T. A., Jr., 1954, Mississippian system of Andrews and Gaines counties, Texas [Unpublished MS thesis]: The University of Texas at Austin, 56 p.
- Bjorlykke, K., 2010, Source rocks and petroleum geochemistry, *in* Bjorlykke, K., ed., Petroleum geoscience: From sedimentary environments to rock physics: Springer, Berlin, Germany, p. 339-349.
- Broadhead, R.F., 2009, Mississippian strata of southeastern New Mexico: distribution, structure, and hydrocarbon plays: New Mexico Geology, v.31, p. 65-71.
- Candelaria, M.P., 1990, "Atoka" detrital a subtle stratigraphic trap in the Midland Basin, *in* Flis, J.E., and Price, R. C., eds., Permian Basin oil and gas fields; innovative ideas in exploration and development: West Texas Geological Society, v. 90-87, p.104-106.
- Craig, L.C., and Connor, C.W., Coordinators, 1979, Paleotectonic Investigations of the Mississippian System in the United States, U.S. Geological Survey Professional Paper 1010, Part III.
- Frenzel, H.N., and 13 others, 1988, The Permian basin region, *in* Sloss, L.L., ed., Sedimentary Cover-North American Craton; U.S.: Geological Society of America, The Geology of North America, Boulder, Colorado, v. D-2 p. 261-306.
- Galley, J.E., 1958, Oil and geology in the Permian Basin of Texas and New Mexico, *in* Weeks, L.G., ed., Habitat of oil: American Association of Petroleum Geologists, Tulsa, Oklahoma, p. 395-446.
- Gutschick, R., and Sandberg, C., 1983, Mississippian Continental Margins on the Conterminous United States, *in* Stanley, D.J. and Moore, G.T., eds., The Shelf break: Critical Interface on Continental Margins: Society of Economic Paleontologist Mineralogists, Tulsa, Oklahoma, Special Publication 33, p. 79-96.

- Hamilton, D.C., and Asquith, G.B., 2000, Depositional, diagenetic, and production histories of Chester ooid grainstones in the Austin (Upper Mississippian) Field: Lea County, New Mexico, *in* DeMis, W., Nelis, M., and Trentham R.C., eds., *The Permian Basin: Proving Ground for Tomorrow's Technologies*, West Texas Geological Society, Publication 00-109, p. 95-105.
- Heslop, K.A., 2010, Generalized Method for the Estimation of TOC from GR and Rt, AAPG Datapages/ Search and Discovery, #80117.
- Hills, J.M., 1984, Sedimentation, tectonism, and hydrocarbon generation in Delaware basin, West Texas and southeastern New Mexico: *American Association of Petroleum Geologists Bulletin*, v. 68, p. 250-267.
- IHS Energy, 2011, Permian Basin Production Data, accessed from PI Dwight, (July, 2011).
- King, P.B., 1948, *Geology of the southern Guadalupe Mountains, Texas*: U.S. Geological Survey Professional Paper 251, 183 p.
- Kinley, T.J., *Geology and hydrocarbon potential of the Barnett shale (Mississippian) in the northern Delaware Basin, West Texas and Southeastern New Mexico* [M.S. thesis]: Texas Christian University, Ft. Worth, 81 p.
- Miall, A.D., 2008, The southern midcontinent, Permian Basin, Ouachitas, *in* Miall, A.D., ed., *The sedimentary basins of the United States and Canada*: Elsevier B.V., Amsterdam, The Netherlands, p. 297-327.
- Ruppel, S.C., and Kane, J., 2006, The Mississippian Barnett Formation: A source-rock, seal, and reservoir produced by early Carboniferous flooding of the Texas craton: http://www.beg.utexas.edu/resprog/permianbasin/PBGSP_members/writ_synth/Mississippian_chapter.pdf (September, 2011).
- Scholle, P., 2006, An introduction and virtual field trip to the Permian reef complex, Guadalupe and Delaware Mountains, New Mexico-West Texas: <http://geoinfo.nmt.edu/staff/scholle/guadalupe.html> (October 2011).
- Serra, O., ed., 1990, *Element, Mineral, Rock Catalog*, Schlumberger.
- Wright, W.F., 1979, *Petroleum geology of the Permian Basin*: West Texas Geological Society, Midland, TX, 98 p.
- Wright, W., 2006, Depositional history of the Atokan Succession (Lower Pennsylvanian) in the Permian Basin: http://www.beg.utexas.edu/resprog/permianbasin/PBGSP_members/writ_synth/Atoka.pdf (August, 2011).
- Ye, H., Royden, L., Burchfiel, C., and Schuepbach, M., 1996, Late Paleozoic deformation of interior North America; the greater ancestral Rocky Mountains: *American Association of Petroleum Geologists Bulletin*, v. 80, p. 1397-1432.

Appendix I. Geochemical Report From the Fasken Fee BM #1 SWD

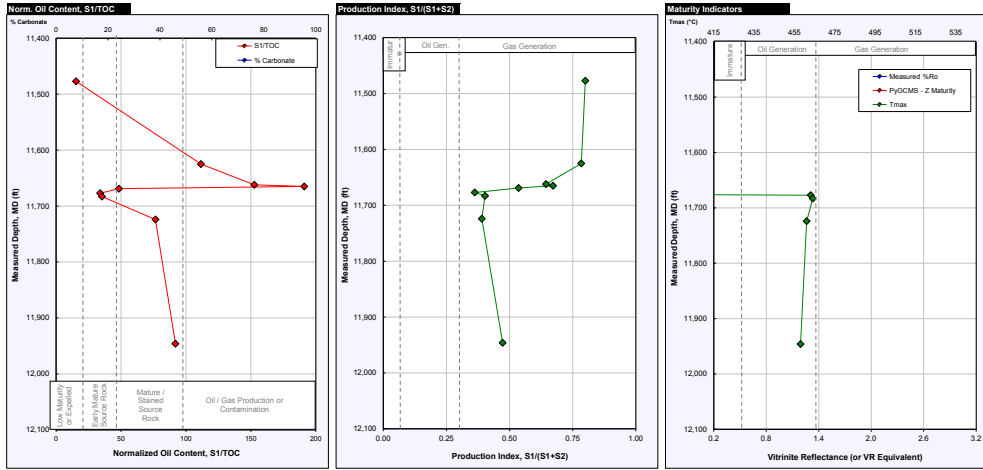


Figure I 1. Geochemical logs for BM SWD #1 well

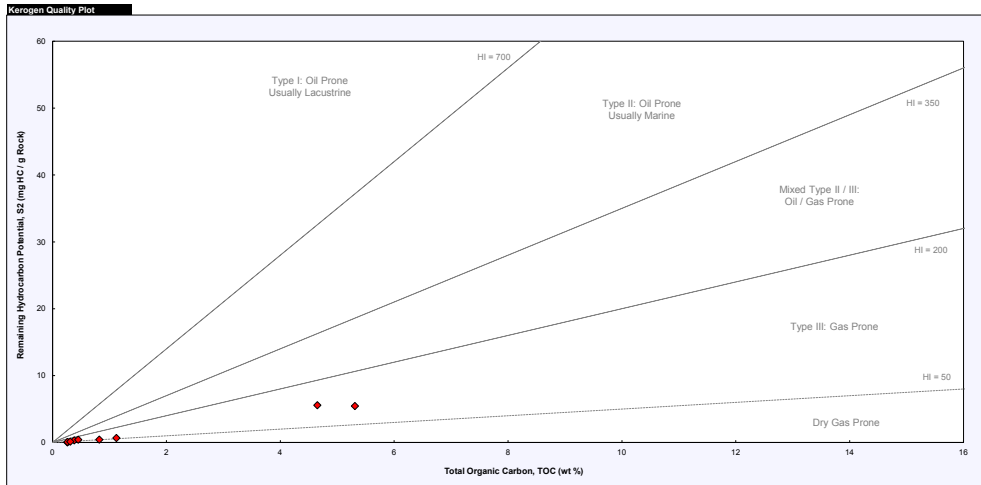


Figure I 2. Kerogen quality relative to TOC Vs. hydrocarbon potential for the BM SWD well

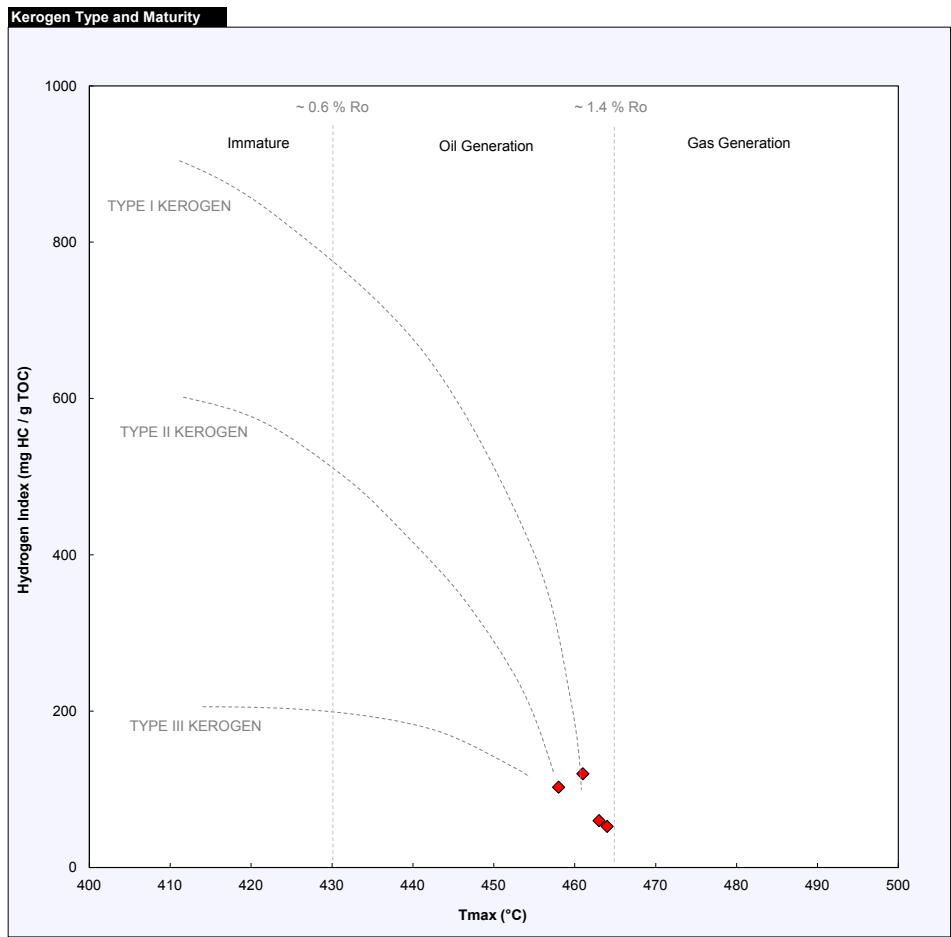


Figure I 3. Kerogen type and maturity based on hydrogen index and Tmax.

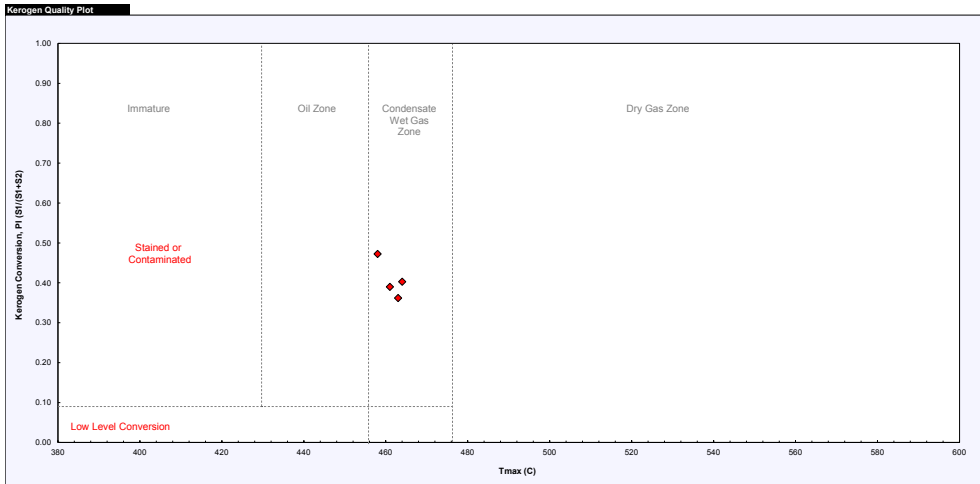


Figure I 4. Kerogen quality plot for the BM SWD #1 well

Vita

Personal Background

Clark Harrison Osterlund
Fort Worth, Texas
Born May 18, 1988, Midland, TX
Son of David and Eve Osterlund

Education

Bachelors of Science in Geology, 2010
Baylor University, Waco, TX

Master of Science in Geology, 2012
Texas Christian University, Fort Worth, TX

Experience

Intern Geologist, summers 2007-2011
Fasken Oil and Ranch Ltd. Midland, TX

Intern Geologist, 2011-2012
BOPCO Ltd., Fort Worth TX

Professional Memberships

American Association of Petroleum Geologists (AAPG)
West Texas Geological Society (WTGS)

ABSTRACT

THE BARNETT SHALE (MISSISSIPPIAN) IN THE CENTRAL MIDLAND BASIN, (ANDREWS, ECTOR, MARTIN, AND MIDLAND COUNTIES)

By Clark H. Osterlund, M.S., 2012
Department of Geology, Energy, and the Environment
Texas Christian University

Dr. Helge Alsleben – Professor of Geology
Dr. R. Nowell Donovan – Professor of Geology, and Provost
Stonnie Pollock – Geologist, Fasken Oil and Ranch Ltd.

Fine-grained units underlying the Atoka Lime Formation in the Midland Basin have historically been interpreted as Pennsylvanian (Atokan) or Mississippian (Chesterian) strata. Recent palynology data suggest that the shale was deposited during the late Mississippian (Osagean-Chesterian), making it equivalent to the Barnett Shale. The trend of the Barnett was studied in a 25-mi² (~65 Km²) area in the Central Midland Basin.

In the study area, siliceous-calcareous units comprising the Barnett shale can be divided into an upper and lower unit. The upper unit can be further subdivided into six subunits by log curve markers, interpreted as gravity-flow deposits consisting of silty bioclastic debris. Isopach maps of the flow deposits suggest a source to the north. Preliminary TOC analyses suggest that the upper Barnett section is relatively TOC lean, whereas the lower Barnett has higher values. Exploration focus can be enhanced by detailed mapping of flows for the upper Barnett.